





## Flexoelectricity in oxide thin films

Guoyang Shen <sup>\*</sup>, Renhong Liang <sup>\*</sup>, Zhiguo Wang <sup>\*</sup>,  
Zhiyong Liu<sup>†</sup> and Longlong Shu <sup>\*</sup>,<sup>‡</sup>,<sup>§</sup>

<sup>\*</sup>School of Physics and Materials Science  
Nanchang University  
Nanchang 330031, P. R. China

<sup>†</sup>School of Materials Science and Engineering  
Nanchang Hangkong University, Nanchang 330063, P. R. China

<sup>‡</sup>zgwang@ncu.edu.cn  
<sup>§</sup>llshu@ncu.edu.cn

Received 5 August 2023; Revised 8 October 2023; Accepted 27 October 2023; Published 18 November 2023

Flexoelectric effect describes the electromechanical coupling between the strain gradient and its internal polarization in all dielectrics. Despite this universality, the resulting flexoelectric field remains small at the macroscopic level. However, in nano-systems, the size-dependent effect of flexoelectricity becomes increasingly significant, leading to a notable flexoelectric field that can strongly influence the material's physical properties. This review aims to explore the flexoelectric effect specifically at the nanoscale. We achieve this by examining strain gradients generated through two distinct methods: internal inhomogeneous strain and external stimulation. In addition, advanced synthesis techniques are utilized to enhance the properties and functionalities associated with flexoelectricity. Furthermore, we delve into other coupled phenomena observed in thin films, including the coupling and utilization of flexomagnetic and flexophotovoltaic effects. This review presents the latest advancements in these areas and highlights their role in driving further breakthroughs in the field of flexoelectricity.

**Keywords:** Flexoelectric effect; strain gradient; polarization; nano-thin film; flexomagnetic; flexophotovoltaic.

### 1. The concept of Flexoelectric Effect

The flexoelectric effect describes the electric polarization induced by strain gradients. The strain gradient fundamentally breaks the inversion symmetry within the crystal, resulting in relative atomic displacements within the lattice. This deformation leads to an asymmetric relative displacement and redistribution of ion charges, resulting in the generation of net charges and subsequent internal polarization, as shown in Fig. 1. Hence, the flexoelectric effect is universally exhibited in dielectric materials regardless of their lattice symmetry, potentially leading to intriguing phenomena, such as the observation of flexoelectricity in nonpiezoelectric materials.<sup>1</sup>

Generally, the flexoelectric effect in dielectric materials can be written as<sup>2</sup>

$$P_l = \mu_{ijkl} \frac{\partial u_{ij}}{\partial x_k}, \quad (1)$$

where  $P_l$  is the induced polarization,  $\partial u/\partial x$  is the strain gradient component and  $\mu_{ijkl}$  is the direct flexoelectric coefficient with respect to strain gradient, a fourth rank tensor.

### 2. A Brief History of Flexoelectric Development

Flexoelectricity refers to the electromechanical coupling phenomenon wherein an electric field is generated by a strain gradient. The theoretical prediction of this effect was made by Kogan in 1964,<sup>3</sup> who proposed that the polarization induced by piezoelectric materials is not solely determined by material deformation, but also by the spatial derivative of strain, i.e., the strain gradient, for center-symmetric crystals subjected to nonuniform deformation, only strain gradient contributes to the polarization. Experimental confirmation of the flexoelectric effect was provided by Bursian and Zaikovskii in 1968.<sup>4</sup> Tagantsev's<sup>5</sup> work in the 1980s further delved into the investigation of flexoelectricity in crystalline materials and revealed that the flexoelectric coefficient is directly proportional to the dielectric constant of the material. Initially, early researchers believed that the flexoelectric coefficient in solid dielectrics was negligibly small, ranging from  $10^{-10}$  C/m to  $10^{-11}$  C/m. However, in the 2000s, Cross *et al.*<sup>6,7</sup> conducted studies on flexoelectricity in various piezoelectric materials and discovered a significant enhancement of the flexoelectric coefficient (around  $10^{-6}$  C/m) in relaxor

<sup>¶</sup>Corresponding authors.

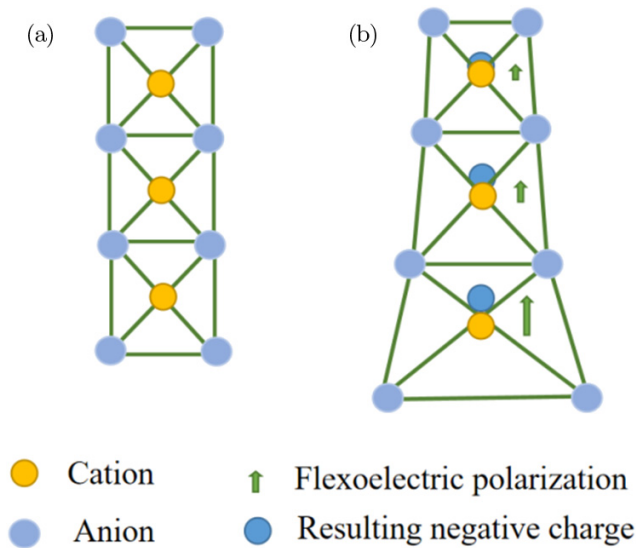


Fig. 1. Origin of flexoelectric effect in crystals. (a) Structure of elementary charges without dipole moment. (b) Under inhomogeneous deformation, a dipole moment via the flexoelectric effect was induced within the unit cell.

ferroelectric lead magnesium niobate (PMN) ceramics. Consequently, the flexoelectric effect in solid materials started to receive increased attention. The presence of grain boundaries, polarity, or surface piezoelectricity in bulk materials introduces complexities when attempting to measure the pure flexoelectric effect. Distinguishing the flexoelectric effect from other contributing factors during experimental measurements becomes challenging due to the influence of grain boundaries. Therefore, the identification and isolation of the pure flexoelectric effect pose experimental difficulties. In the 2004s, Zubko *et al.*<sup>8</sup> conducted a comprehensive investigation of the flexoelectric effect in single-crystal bulk strontium titanate using a mechanical bending method. Through carefully designed experiments, they successfully demonstrated the presence of strain gradient-induced polarization, confirming the existence of the flexoelectric effect in solid bulk materials. Strain engineering techniques leverage substrate-induced stress to modify the properties of thin films, utilizing the coupling between strain gradients and polarization to achieve performance modifications. Starting from

2011, Catalan *et al.*<sup>9,10</sup> conducted studies on the strain distribution in ferroelectric PbTiO<sub>3</sub> epitaxial films and PbZrO<sub>3</sub>-based anti-ferroelectric thin films. By relieving the mismatch with the substrate through domain formation, they proposed a novel physical technique that exploits the coupled flexoelectric effect, capable of inducing polarization rotation in amorphous ferroelectric materials. In 2012, Lu *et al.*<sup>11</sup> employed atomic force microscopy (AFM) to investigate the phenomenon of ferroelectric domain polarization direction reversal induced by the flexoelectric effect in heterogeneous films of BaTiO<sub>3</sub> (BTO). In 2018, Yang<sup>12</sup> found that non-piezoelectric SrTiO<sub>3</sub> crystals exhibit a tendency to generate local strain gradients when subjected to an atomic force microscope (AFM) tip. This localized generation of strain gradients leads to local flexoelectric polarization, which has a significant impact on the photovoltaic effect observed in SrTiO<sub>3</sub> crystals. Building upon this work, Shu *et al.*<sup>13</sup> proposed a novel phenomenon known as the “photoflexoelectric effect” in 2020. They put forward the idea that light absorption can be utilized to enhance the flexoelectric response. Through experimental evidence, they demonstrated the existence of photoflexoelectricity in halide perovskite materials. Under illumination, these materials exhibited effective flexoelectric coefficients several orders of magnitude larger than those observed in the absence of light. In recent years, an increasing number of studies have focused on investigating the flexoelectric effect in two-dimensional (2D) materials.<sup>14–16</sup> These materials possess remarkable flexibility, and simple bending induces significant strain gradients. Additionally, advancements in self-supporting thin-film fabrication techniques<sup>17,18</sup> have further expanded the range of applications for 2D materials. The progress in these field, as depicted in Fig. 2, highlights the immense potential of the flexoelectric effect in semiconductor electronics and optoelectronic devices.

### 3. Flexoelectric Effect at Nanometer Scale

Despite the universality of the flexoelectric effect, its resulting field at the macroscopic level remains relatively small. For instance, the strain gradient achievable through mechanical bending of a bulk solid does not exceed  $10^{-1} \text{ m}^{-1}$ , resulting in a flexoelectric polarization of about  $10^{-9} \mu\text{C cm}^{-2}$

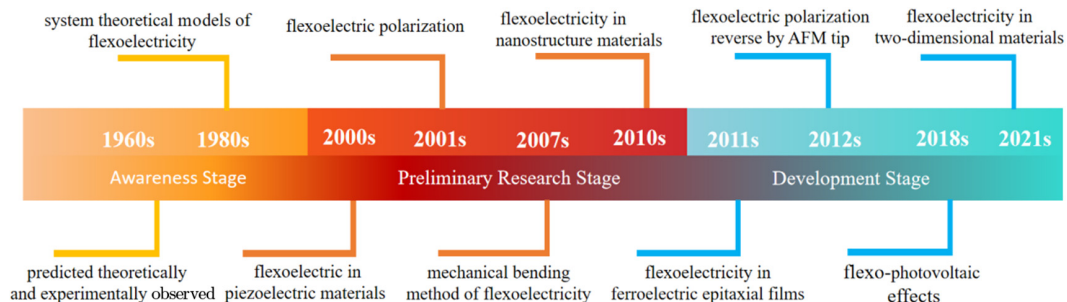


Fig. 2. Time line illustrating the major milestones in the investigation of the flexoelectric effect.

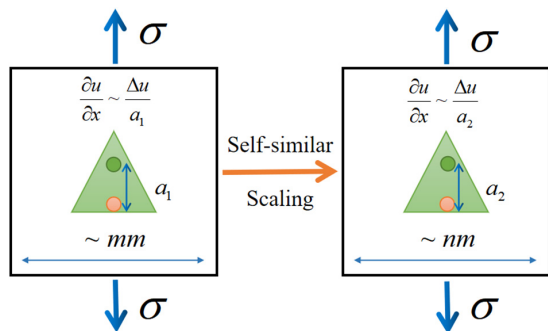


Fig. 3. Schematic diagram of the size effect of flexoelectricity.

(compared to piezoelectric polarization ( $\sim 10^{-1} \mu\text{C cm}^{-2}$ ) which is essentially negligible).<sup>19–22</sup> However, when the material dimensions are scaled down to the nanometer range, the magnitude of the strain gradient becomes significantly pronounced due to its inverse relationship with the lattice relaxation length, as shown in Fig. 3. For instance, a strain change of 1% within a 10 nm range yields a substantial strain gradient of  $10^6 \text{ m}^{-1}$ .<sup>14,23</sup> The induced flexoelectric field can reach significant magnitudes that affect the material's physical properties. For example, in epitaxial thin films, strain can be generated due to lattice mismatch at the interfaces, and this strain has been found responsible for modifying the phase diagram<sup>24,25</sup> and shifting the transition temperature.<sup>20,26</sup> However, strain itself cannot fully explain the observed differences in properties between bulk materials and thin films. Studies have indicated that strain gradients also influence polarization and are accountable for the observed dielectric peak smearing. However, it is important to note that the estimation of this strain gradient is based on numerical calculations of the lattice parameter change, as the fundamental challenge of directly measuring flexoelectric coefficients in thin films remains unresolved. Unlike the methods employed in bulk material studies,<sup>2,8</sup> direct measurements of flexoelectricity in thin films face difficulties due to their attachment to rigid substrates with strong chemical bonds.<sup>27,28</sup> Consequently, the development of accurate theoretical models becomes crucial in providing guidance for the estimation of strain gradients.

According to phenomenology, strain gradient generates an internal electric field  $E_s$  due to the flexoelectric effect,<sup>2,29,30</sup> which can be expressed as follows:

$$E_s = \frac{e}{4\pi\epsilon_0 a} \frac{\partial u}{\partial x}, \quad (2)$$

where  $e$  is the electronic charge,  $\epsilon_0$  is the permittivity of free space,  $a$  is the lattice parameter of the unstrained ferroelectric material, and  $\partial u/\partial x$  is the strain gradient. Lee<sup>23</sup> estimated  $E_s$  in tensile-strained  $\text{HoMnO}_3$  epitaxial thin film as a model system by inserting the experimental values of  $\partial u/\partial x$  into Eq. (2) and found that  $E_s \sim 5.0 \text{ MV m}^{-1}$  in  $\text{HoMnO}_3$  at room temperature. Comparing this value with the room temperature ferroelectric coercive field of approximately  $40 \text{ MV m}^{-1}$  in

$\text{HoMnO}_3$  thin films, the estimated  $E_s$  appears relatively small. However, it should be noted that the coercive field significantly decreases toward temperatures close to the Curie temperature ( $T_c$ ), where the ferroelectric interaction becomes weaker.<sup>31</sup> Moreover, bending the thin film can induce a larger strain gradient.<sup>32</sup> As a result,  $E_s$  can become comparable to the coercive field, and the associated flexoelectric effect can become notably significant.

Therefore, understanding and controlling the flexoelectric effects of composite oxide films at the nanoscale is crucial for the future development of nanotechnology and electronics. In recent years, advancements in thin film fabrication techniques have enabled the synthesis of diverse complex structured thin films, such as heterojunction epitaxial growth, superlattices, and ultra-thin films. For instance, Tang *et al.*<sup>33</sup> have successfully grown epitaxial  $\text{PbTiO}_3$  thin films on  $\text{SrTiO}_3$  substrates, resulting in a compressive strain along the in-plane direction due to lattice mismatch between the film and the substrate. Ferroelectric displacement mapping techniques have revealed a monoclinic distortion within the compressed  $\text{PbTiO}_3$  film, exhibiting a polarization exceeding  $50 \mu\text{C/cm}^2$ . Epitaxial heterostructures offer multiple interfaces and boundaries where significant strain gradients can be generated. Xu *et al.*<sup>34</sup> investigated the flexoelectric modulation of surface potential in  $\text{LaFeO}_3$  (LFO) thin films through heterostructures. By manipulating the epitaxial layer-substrate mismatch, they achieved LFO thin films with and without the flexoelectric effect as the large mismatch strain gradually relaxed with increasing thickness. Furthermore, X-ray photoelectron spectroscopy analysis revealed that the flexoelectric polarization altered the energy band alignment and modified the interfacial potential barrier of the LFO layer. Furthermore, higher strain gradients ranging from  $10^6 \text{ m}^{-1}$  to  $10^8 \text{ m}^{-1}$  can be achieved by utilizing scanning probe microscopy (SPM) tips<sup>11,35–42</sup> to press the surface of the film. Zhao *et al.*<sup>43</sup> mechanically induced out-of-plane domains in 10 nm  $\text{Hf}_{0.5}\text{Zr}_{0.5}\text{O}_2$  (HZO) ferroelectric films at room temperature using strain gradients generated by the AFM tip. This nondestructive approach avoids charge injection by mechanical etching and thus reveals the true polarization state. These findings pave the way for the broader utilization of flexoelectricity and the realization of ultra-high-density storage in HZO films. The implications of these advancements extend beyond merely increasing the flexoelectric field; they provide a solid foundation for great potential of the flexoelectric effect in electronic applications, such as energy harvesting,<sup>44–46</sup> actuators and sensor,<sup>47,48</sup> photodetectors,<sup>49</sup> crack-monitoring sensors,<sup>50</sup> nanogenerators,<sup>51</sup> etc.

Meanwhile, other physical properties related to flexoelectric effect, such as flexomagnetic (FIM) effect and flexophotovoltaic (FPV) effect, have received extreme attention. For example, Lukashov<sup>52</sup> demonstrated the linearity of the flexomagnetic effect and utilized first-principles calculations to determine a flexomagnetic coefficient of approximately  $\sim 2 \mu_B \text{ \AA}$  in the antiperovskite  $\text{Mn}_3\text{GaN}$ . Subsequently,

Table 1. Experimental and calculated values of strain gradient for thin film materials.

Source types	Sources of strain gradient	Values of strain gradient ( $m^{-1}$ )	Ref.
Lattice mismatch	HoMnO <sub>3</sub> /Pt (111)/Al <sub>2</sub> O <sub>3</sub> (0006)	$10^5 \sim 10^6$	23
	BTO/LSMO film	$\sim 10^5$	38
	BVO/YSZ film	$\approx 5 \times 10^6$	66
	PTO/LSAT (101)	$\sim 10^6$	67
	BFO/NGO (NdGaO <sub>3</sub> )	$\sim 10^6$	77
By bending	BFO membranes	$5.2 \times 10^6 \sim 3.5 \times 10^7$	129
	Pt/BFO/LSMO devise	$4 \times 10^4 \sim 1 \times 10^5$	132
	PTO/STO	$\sim 4 \times 10^6$	84
Phase boundary	S-BFO/T-BFO mixed-phase boundary on LaAlO <sub>3</sub> (LAO)	$\sim 3.3 \times 10^7$	87
Needle tip press	AFM tip/SrTiO <sub>3</sub> single crystals	$> 10^6$	12
	AFM tip/SrTiO <sub>3</sub> (3.5 nm) film	$\sim 10^7$	42
	AFM tip/SrTiO <sub>3</sub> (3.9 nm) film	$\sim 10^7$	106

Sidhardh and Ray<sup>53</sup> investigated the theoretical modeling of the flexomagnetic effect within a piezomagnetic nanobeam subjected to bending. They derived tensor control equations and established associated boundary conditions for mechanical and magnetic variables employing the variational principle. Furthermore, Yang *et al.*<sup>12</sup> found the FPV effect in the centrosymmetric structures of simple crystals SrTiO<sub>3</sub> and TiO<sub>2</sub>. Notably, they observed that the photovoltaic current ( $I_{pv}$ ) increased by 100 times as the loading force rose from 1  $\mu$ N to 15  $\mu$ N, thus demonstrating the potential of the FPV effect as a means to enhance the performance of solar cells and photovoltaic devices. Since then, significant attention has been devoted to exploring the FPV effect whereby the photovoltaic current can be modulated through flexoelectricity. As one of the typical representatives of lead-free perovskite ferroelectric materials, bismuth ferrate (BiFeO<sub>3</sub>) has a narrow band gap (2.2–2.8 eV) and large ferroelectric polarization (exceeding 100  $\mu$ C/cm<sup>2</sup>). In recent years, significant progress has been made in studying the photovoltaic effect in BiFeO<sub>3</sub> ferroelectric materials.<sup>54–58</sup> It has been shown that flexoelectricity in these materials can induce the separation of photogenerated carriers and alter the distribution of interfacial barriers,<sup>42</sup> thereby influencing the mechanical modulation of ferroelectric quantum tunneling effects. For instance, the combination of oxygen vacancy gradient distribution and flexoelectric effect,<sup>59</sup> as well as the interfacial dislocation-mediated light-modulated electrical transport behavior,<sup>60</sup> have been observed. Moreover, the strain gradient in BiFeO<sub>3</sub> films can be greatly enhanced by ultrafast photoexcitation, opening up possibilities for the direct coupling of flexoelectricity with optical stimulation.<sup>61</sup> Additionally, the flexoelectric effect has been found to significantly modulate the electrical transport properties of the interfacial two-dimensional electron gas (2DEG) in LaAlO<sub>3</sub>/SrTiO<sub>3</sub> heterostructures.<sup>62</sup> These advancements demonstrate the considerable potential for utilizing the flexoelectric effect in nanooptoelectronic devices. Notably, there are numerous sources of flexoelectric effects induced by strain gradients in nanosized oxide films. These effects can originate from internal inhomogeneous deformations, such

as lattice mismatch between the film and the substrate, spontaneous polarization of ferroelastic domain walls, mismatch dislocations, and strain relaxation behavior. External stimuli, such as large local strain gradients generated by SPM tip pressure. Table 1 summarizes the various types of strain gradients in real materials, providing a diverse platform for exploring flexoelectricity and its related properties.

In 2019, Shu's group<sup>63</sup> reviewed recent research advances in flexoelectric effects, mainly focusing on flexoelectric materials in bulks and related applications. In this paper, we particularly highlighted the various primary sources of flexoelectric effects induced by strain gradients in nanoscale thin films. The review outlined the experimental progress in studying these effects and briefly discussed their relevant properties, which are very important for a more comprehensive understanding and utilization of flexoelectricity.

## 4. Flexoelectric Effects in Thin Films

### 4.1. Strain gradient induced flexoelectric effects on thin film

#### 4.1.1. From mismatch strain between film and substrate

In epitaxial oxide films, the presence of lattice mismatch between the film and substrate leads to strain relaxation at the interface, resulting in the formation of strain gradients within a tens-of-nanometer range, as shown in Fig. 4(a). The mismatch strain typically relaxes exponentially across the epitaxial film, with the average strain gradient reaching magnitudes up to  $10^6 m^{-1}$ .<sup>23,64,65</sup> Notably, this value is approximately six to seven orders of magnitude larger compared to the corresponding bulk solid value. Consequently, the flexoelectric effects induced by the strain gradients arising from the lattice mismatch can significantly impact the physical properties of epitaxial films. These effects encompass domain structure control and imprinting,<sup>23</sup> configuration of defects,<sup>66,67</sup> and continuous rotation of the spontaneous polarization direction.<sup>9</sup>



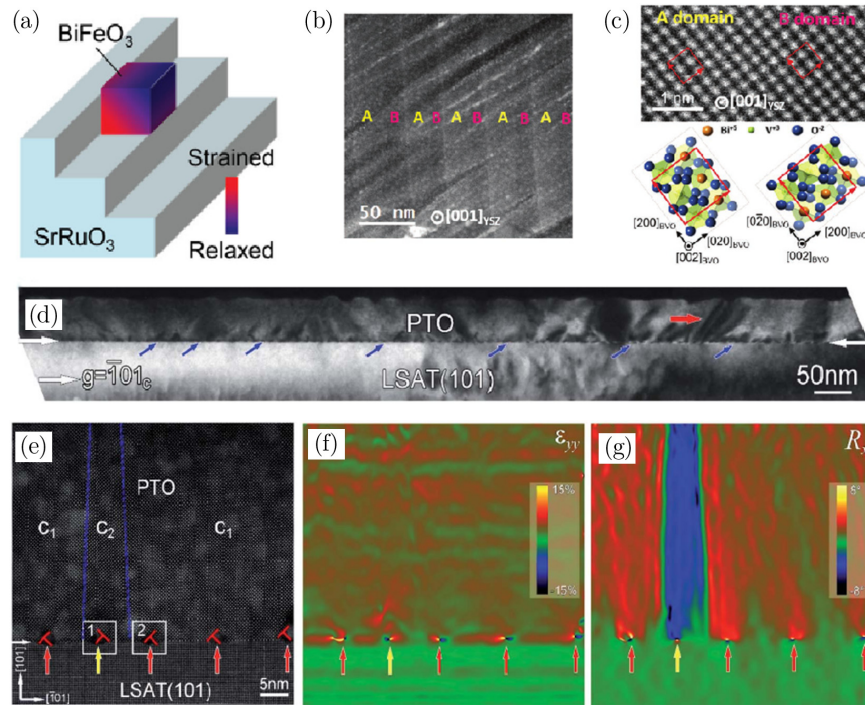


Fig. 4. (Color online) (a) Schematically describe the expected strain profile for  $\text{BiFeO}_3/\text{SrRuO}_3/\text{SrTiO}_3$  structure. (b) Plane-view HAADF-STEM image at the surface of BVO/YSZ film. (c) High-resolution plane-view HAADF-STEM images taken along the  $[001]$  YSZ, and a schematic diagram of unit cells of A domain and B domain. The red boxes represent monoclinic unit cells of these domains. (d) Two-beam dark-field image obtained near the  $[010]$  zone axis of LSAT, showing the high-density of defects at the PTO/LSAT (101) interface. (e) Low-magnification high-resolution HAADF-STEM image of a 50 nm PTO/LSAT (101) thin film. (f), (g) Strain distribution corresponding to the area of (e), (f) out-of-plane strain ( $\epsilon_{yy}$ ), and (g) lattice rotation ( $R_x$ ). Note the same lattice rotation direction between the stripe  $90^\circ$  domains and misfit dislocations.

The exploration of polar domain emergence in ferroelectrics has been extensively investigated over the past decades.<sup>54,55,68,69</sup> Various sources of built-in electric fields in real materials,<sup>70–72</sup> including but not limited to piezoelectric effects, interface polarization effects, and defects, have been identified as factors influencing the conformation of ferroelectric domains. Generally, flexoelectricity has limited influence due to its small coefficients, however, the situation changes in nanosized ferroelectric film systems, where the internal field generated by flexoelectricity can dominate the internal field from other sources under certain conditions. Due to the clamping effect between the film and the substrate, stress tends to accumulate in the film. Consequently, the in-plane shear strain gradient induces the flexoelectric effect, resulting in a decrease in the symmetry of the domain wall region, which is released by forming alternating A and B domains with different orientations,<sup>66</sup> as depicted in Figs. 4(b) and 4(c). As aforementioned, the ferroelectric coercivity becomes weaker at high temperatures during the deposition of the film, while the strain gradient remains almost constant. Therefore, the flexoelectric effect decisively affects the ferroelectric domain configuration of the grown ferroelectric film.

During the growth of ferroelectric oxide films on substrates, lattice mismatch is inevitable. When the lattice

mismatch exceeds a critical value or the film reaches a critical thickness, defects such as point defects, dislocations, and defective dipoles are formed. Figure 4(d) illustrates the formation of mismatch dislocations, which generally result in polarization instability and degradation of the out-of-plane piezoelectric response.<sup>73,74</sup> The presence of mismatch dislocations induces several effects. First, the strain around the dislocation core creates a significant local polarization gradient, leading to strong flexoelectric field near the core and subsequently suppressing the ferroelectric polarization in that region. Additionally, the interaction between the flexoelectric-coupled ferroelastic domains and mismatch dislocations leads to the pinning of ferroelastic domain walls. This pinning restricts the motion of these domain walls under an applied electric field, reducing the extrinsic contribution to the piezoelectric response and causing a shift in the hysteresis loop.<sup>75</sup> Furthermore, the evolution of ferroelectric thin films can be controlled by adjusting the deposition temperature and film thickness. Jeon *et al.*<sup>76</sup> tuned the diode effect and the variation of the hysteresis loop by means of the strain relaxation-induced flexoelectric field of films with different thicknesses. This control was achieved by manipulating the distribution positions of defect layers at different temperatures and arranging defect dipoles. Notably, the formation of mismatch dislocations (Fig. 4(e)) generates larger strain

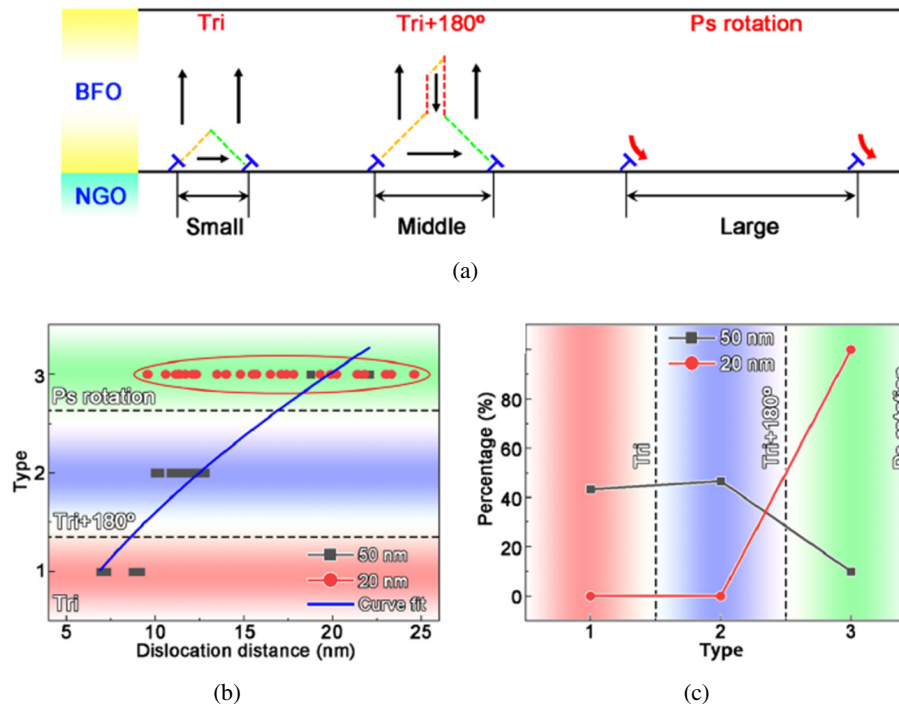


Fig. 5. Flexoelectric behaviors in BiFeO<sub>3</sub> films with different thicknesses. (a) The schematic of flexoelectric responses with different dislocation spacings. (b) Different flexoelectric behaviors as a function of dislocation distances. (c) The percentages of different flexoelectric behaviors.

gradients around the dislocation core, which triggers polarization rotation<sup>67</sup> (Figs. 4(f) and 4(g)). Furthermore, dislocation spacing can modulate the flexoelectric behavior of the film. Thinner BFO films manifest as asymmetric polarization rotations around individual dislocations, but these strain fields are highly correlated. As the dislocation spacings increase, a transition in flexoelectric behavior occurs, progressing from triangular-like nanodomains (type 1) to 180° domains positioned above the triangular-like nanodomains (type 2) and eventually resulting in polarization rotation (type 3).<sup>77</sup> This transition is depicted in Figs. 5(a)–5(c) and arises from out-of-plane positive and shear strains observed in the horizontal gradients between adjacent dislocations. The inclusion of misfit dislocations or dislocation networks in ferroelectric thin films induces alterations in the local strain. Subsequently, the interaction between the local strain and ferroelastic domain strain leads to modifications in the polarization distribution and the pinning of domain walls.

In conventional thin films, the attachment to strong-chemical-bond<sup>27</sup> substrates introduce strains and strain gradients in the film when bending occurs. This leads to the generation of piezoelectricity, even in films that are nominally nonpiezoelectric, thereby masking the true flexoelectric effect.<sup>78</sup> To address this issue, Shu *et al.*<sup>79</sup> proposed and demonstrated epitaxial flexoelectric films that utilize weak van der Waals forces at the interface, thereby eliminating the clamping effect from the substrate. This approach enables the measurement of the intrinsic flexoelectric coefficient by

bending the substrate. Moreover, the weak van der Waals force can be utilized to peel off and transfer the epitaxial film onto different substrates, providing opportunities for the application of complex oxides in devices.<sup>80</sup>

#### 4.1.2. From the interface and phase boundaries

Interfaces are commonly present in thin films, and nanoscale characterization has revealed the existence of significant inhomogeneous strain,<sup>81,82</sup> as shown in Figs. 6(a)–6(c). The nonuniform strain within these interfaces gives rise to unique structures and properties through the flexoelectric effect. These effects include the attainment of a zero Poisson's ratio state,<sup>33</sup> enhanced ferroelectricity,<sup>16,20,26</sup> the stabilization of new ferroelectric phases,<sup>83</sup> and the presence of polar topological defects.<sup>84–86</sup> The nonuniformly strained interfaces primarily include mixed-phase boundaries and surfaces. Moreover, the macroscopic-scale flexoelectric behavior at interfaces provides new insights for their potential applications.

The strain mismatch in epitaxial thin films serves as an effective means to control the competition between different phases in oxide films.<sup>30</sup> The phase boundaries associated with this strain mismatch often exhibit significant strain gradients, and as a result of the flexoelectric effect, these mixed-phase interfaces showcase intriguing properties. For example, enhanced anisotropic photocurrent,<sup>87</sup> loss of ferroelectric polarization,<sup>88</sup> localized conduction,<sup>89</sup> and multi-ferroic optical control.<sup>90</sup> Researchers Junquera and Ghosez<sup>91</sup>

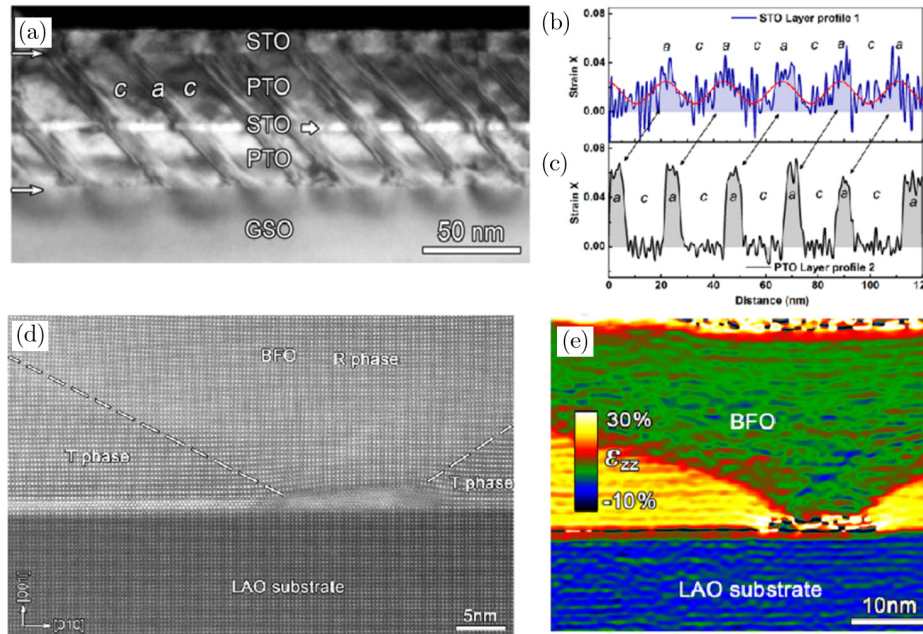


Fig. 6. (a) Dark-field TEM image of the periodic *a/c* domains in the  $\text{SrTiO}_3/\text{PbTiO}_3/\text{SrTiO}_3/\text{PbTiO}_3/\text{GdScO}_3(110)_{\text{orthorhombic}}$  film. Lattice strain X map by GPA. Note the clear lattice change across the *a/c* domains shown in (b) and (c), which correspond to the middle  $\text{SrTiO}_3$  layer and the middle of the top  $\text{PbTiO}_3$  layer, respectively. Lattice in the *c* domains in the middle of the top  $\text{PbTiO}_3$  layer was chosen as a reference, where 0 strain can be readily identified. (d) A higher magnified HAADF-STEM image of the  $\text{BiFeO}_3/\text{LaAlO}_3(001)$  film viewed along  $[100]$ . The domain boundaries between T like and R like  $\text{BiFeO}_3$  are marked by white dotted lines. (e) Out-of-plane strain ( $\epsilon_{zz}$ ) maps via GPA. A LAO substrate is chosen as the reference lattice.

investigated the thickness-dependent ferroelectric properties of BTO thin films sandwiched between metallic  $\text{SrRuO}_3$  electrodes in a short-circuit configuration. They demonstrated that the ferroelectric properties disappear below a critical thickness of approximately six unit cells ( $\sim 24 \text{ \AA}$ ) due to the depolarizing electrostatic field induced by the dipole at the ferroelectric–metal interface. Furthermore, in epitaxial  $\text{BiFeO}_3$  films of moderate thickness. As shown in Figs. 6(d) and 6(e), Tang *et al.*<sup>92</sup> discovered morphotropic phase boundaries (MPB) in the form of T-like and R-like configurations. They observed a mechanical bending deformation in the R-like  $\text{BiFeO}_3$  phase with a strain gradient of  $10^6 \text{ m}^{-1}$ . This large strain gradient at the phase transition boundary can redistribute photoexcited electron–hole pairs to nearby quasi-isotropic phase boundaries, resulting in a significant alteration of the local nonequilibrium carrier density.<sup>86</sup>

Meanwhile, mismatch dislocations, as one of the pathways for releasing mismatch strain, are typically present in elastically strained epitaxial films, where strain gradients naturally exist around the dislocation core due to translational symmetry breaking at the dislocation. These strain gradients have a significant impact on the electrical and mechanical properties of the films. To investigate this effect, Gao *et al.*<sup>93</sup> utilized aberration-corrected scanning transmission electron microscopy (STEM) to directly measure the flexoelectric polarization ( $\sim 28 \mu\text{C}/\text{cm}^2$ ) at the dislocation core in  $\text{SrTiO}_3$ . They observed that the polarized charge can interact with the dislocation core in a nonstoichiometric manner, thereby

influencing the electrical activity in the film. It is evident that achieving tunable flexoelectric behavior in specific thin films remains an ongoing challenge, and interfacial dislocation arrays with high density offer a promising avenue for further research in this field.<sup>73</sup>

Due to the nanoscale dimensions and large specific surface area of ferroelectric films, surface effects play a crucial role and cannot be disregarded. Various surface factors, including surface piezoelectricity, surface bonding environment, and needle tip contact,<sup>94</sup> are expected to induce domain switching. The surface effect is believed to simultaneously adjust both long-range and short-range interactions within ferroelectrics,<sup>95,96</sup> as depicted in Figs. 7(a) and 7(b). Dai *et al.*<sup>97</sup> introduced modifications to the Gibbs surface energy to explain the atomistic results of surface piezoelectricity. They proposed that even nonpiezoelectric materials can exhibit a piezoelectric response due to surface effects. Considering the effects of surface piezoelectricity and flexoelectricity, Shen and Hu<sup>98</sup> developed an electric enthalpy variational principle for nanoscale dielectrics, incorporating flexoelectric effects, surface effects, and electrostatic forces. This variational principle enabled the derivation of governing equations and generalized electromechanical Young–Laplace equations, which account for the influence of flexoelectricity, surface effects, and electrostatic forces. Moreover, pioneering attempts have been made to manipulate ferroelectric domains by exploiting surface effects. Recent studies<sup>23,99</sup> have demonstrated that the application of local mechanical loads to the surface can induce



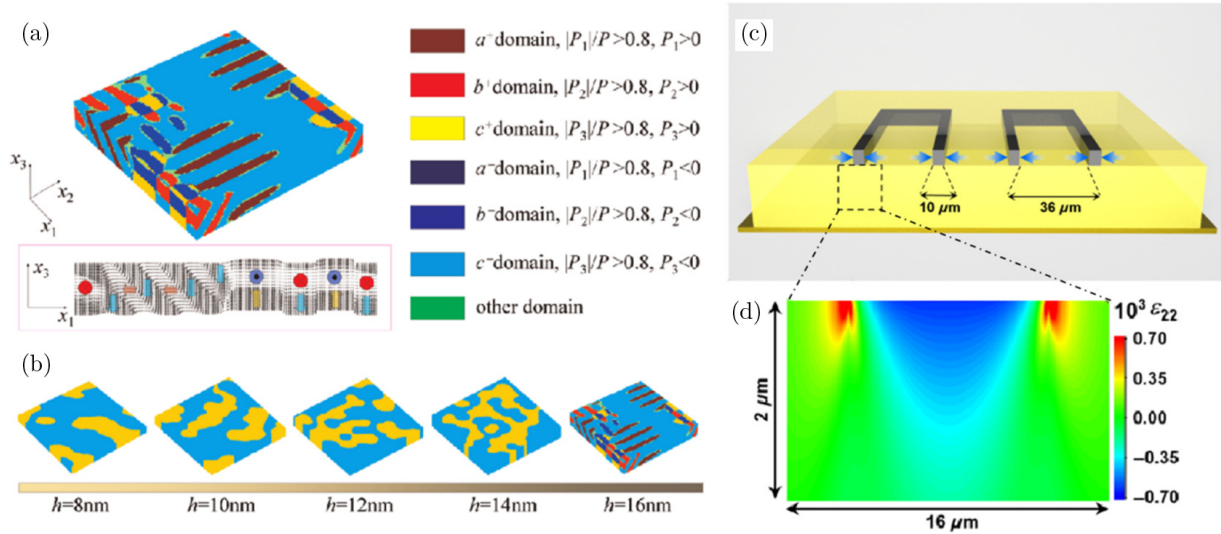


Fig. 7. (Color online) (a) Simulated domain pattern in 16 nm-thick PbTiO<sub>3</sub> nanofilm at room temperature and (b) dependence of the domain pattern on film thickness. (c) Schematic of a cross-section of the PMN-PT substrate, where blue arrows represent the film force. (d) A typical strain distribution in the PMN-PT substrate underneath the metal strip.

significant surface-related effects, leading to the formation of microscopic 180° domains in the vicinity of the loaded region. The domain shift exhibits a size dependence, with a more pronounced effect as the length of the loaded region decreases. Additionally, the surface effect significantly alters the polarization field, and narrower loading areas can suppress the mechanical reversal of ferroelectric polarization.<sup>100</sup>

Localized deposition of stressed films with varying thicknesses introduces nonuniform strains on the surface of ferroelectric films. The presence of compressive (tensile) stress in the thin film causes local expansion (contraction) near the interface, resulting in strain gradients within the ferroelectric lattice. By depositing stressed thin-film strain gauges, a strain gradient is created, enabling the control of flexoelectric properties on a case-by-case basis. This control allows for the continuous regulation of the internal bias, thereby controlling the ferroelastic strain exerted by the ferroelectric phase and achieving control over ferroelastic nonvolatility. As shown in Figs. 7(c) and 7(d), Hou *et al.*<sup>101</sup> successfully achieved precise control of nonvolatile ferroelastic strain by manipulating the stress film deposited on the ferroelectric film. The generation of strain gradients is achieved through the use of stressed thin-film strain gauges, enabling individual control of flexoelectricity. This technology permits continuous adjustment of the internal bias voltage. Furthermore, Zheng *et al.*<sup>102</sup> deposited ZnO thin films on pre-deformed shape memory alloy (SMA), where temperature variations during thermal cycling resulted in surface deformation of the alloy. The inhomogeneous deformation of the ZnO film breaks the center of symmetry of positive and negative charges, leading to the generation of flexoelectric charge output current/voltage. This discovery provides a novel avenue for applying flexoelectric effects on a macroscopic scale.

## 4.2. Strain gradient induced flexoelectric effect from external forces

### 4.2.1. From AFM/PFM needle tip press

By utilizing a AFM tip to exert pressure on the material surface, instead of manipulating intrinsic factors affecting flexoelectric properties, a significant strain gradient can be generated near the surface. Particularly for nanoscale materials, pressing the AFM tip into the material surface can generate a larger strain gradient, reaching values as high as  $10^6$ – $10^7$  m<sup>-1</sup>, as shown in Fig. 8(a). Furthermore, the strain gradient and flexoelectric effect can be intentionally manipulated by repeatedly applying and releasing the stress induced by the AFM tip. In a groundbreaking study, Lu *et al.*<sup>11</sup> experimentally demonstrated the deterministic 180° downward reversal of ferroelectric polarization in BTO films through the application of pressure from an AFM tip. This AFM tip pressing serves as a dynamic tool for precise control of ferroelectric polarization and has initiated extensive investigations into the manipulation of various physical properties, encompassing ferroelectric domains,<sup>38,40</sup> oxygen vacancy concentration,<sup>103–105</sup> and local transport behavior.<sup>41,42,106</sup> Thus, the flexoelectric effect induced by the AFM/PFM tip has exhibited remarkable scientific and technological potential.

By applying pressure from the tip of an AFM onto the surface of ferroelectric thin films, the intense flexoelectric field generated by the strain gradient at the tip can induce reverse polarization and facilitate the writing of domains within the ferroelectric film.<sup>51,107</sup> When the AFM tip is pressed, the ultrathin ferroelectric film experiences compressive strain in both longitudinal and transverse directions. Under compression, the ferroelectric coercivity decreases,



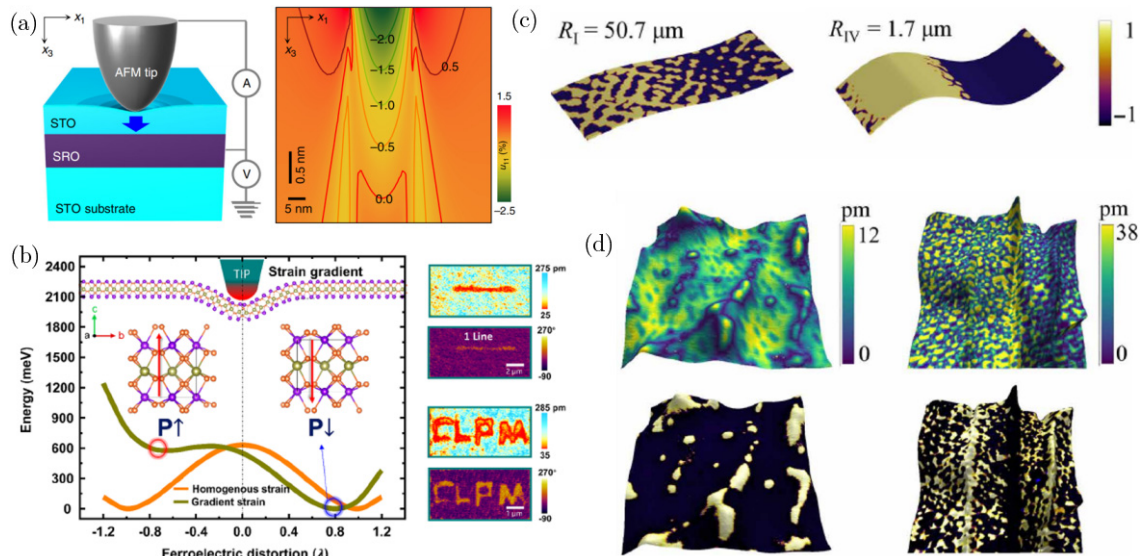


Fig. 8. (Color online) (a) Schematic of the experimental setup, illustrating flexoelectric polarization (blue arrow) generated by the atomic force microscope (AFM) tip pressing the surface of ultra thin SrTiO<sub>3</sub> and simulated transverse strain  $u_{11}$  in a nine unit cell-thick (i.e., 3.5 nm-thick) STO under a representative tip loading force of  $5 \mu\text{N}$ . Along the central line,  $u_{11}$  varies by  $\sim 0.5\%$  within  $\Delta x_3 = 0.5 \text{ nm}$ , yielding  $\partial u_{11}/\partial x_3 \sim 10^7 \text{ m}^{-1}$ ; (b) Potential energy profile and nanoscopic mechanical switching. The calculation for potential energy profile as a function of ferroelectric distortion ( $\lambda$ ) under inhomogeneous strain and homogeneous strain, PFM amplitude and phase images of mechanically written linear domains after pushing the grounded tip along a straight line and a CLPM-pattern functioned by a loading force of  $\sim 450 \text{ nN}$ ; (c) Flexoelectric engineering of CIPS. Phase-field simulation of polarization distribution under different radii of curvature, as revealed by vertical PFM amplitude and phase mappings imposed on 3D AFM topography; (d) Domain evolution associated with topography variation as revealed by vertical PFM amplitude and phase mappings, both imposed on 3D AFM topography.

thereby enabling effective reversal of the ferroelectric polarization direction through the strain gradient. Zhao *et al.*<sup>43</sup> successfully achieved mechanically written out-of-plane domains in HZO ferroelectric thin films by generating strain gradients at the AFM tip, while avoiding charge injection and revealing the true polarization state. Furthermore, they demonstrated the capability to mechanically write and erase specific nanoscale patterns,<sup>108–110</sup> as shown in Fig. 8(b). However, for an extended period, in cases involving tip-induced gradient film structures, pressing the AFM tip onto the ferroelectric film surface would result in a definite distribution of strain gradient. The tip pressing always induces a noticeable downward flexoelectric field, causing the domain path to move solely from an upward to a downward direction, rather than the reverse. Addressing this limitation, Liu *et al.*<sup>111</sup> employed a first-principles simulation approach and proposed a bidirectional reversal scheme based on the distinct roles of the flexoelectric field and the effective dipole field in polarization reversal. They theoretically demonstrated that reversible  $180^\circ$  mechanical swift in the tip-film structure is feasible when the shielding condition of the ferroelectric thin film and the applied tip loading force fall within an appropriate range. Furthermore, traditional ferroelectric domain engineering techniques rely on periodic electric fields, which often result in field-driven phenomena such as ion migration and damage. To mitigate these issues, Ming *et al.*<sup>112</sup> propose a novel approach based on the exploitation of the strong

correlation between polarization and topographic surface variation, thereby eliminating the need for external electric fields. By precisely controlling the radius of curvature of the morphology and employing cyclic mechanical scanning, multiple intermediate polarization states can be achieved. As shown in Figs. 8(c) and 8(d). The authors apply this alternative switching mechanism to CuInP<sub>2</sub>S<sub>6</sub> (CIPS) using the flexoelectric effect and successfully demonstrate the on-demand mechanical modulation of CIPS by manipulating the strain gradient underneath a scanning probe. Consequently, this technique opens up the possibility of engineering multiple polarization states in CIPS without relying on conventional electric field-based methods.

Reverse flexoelectricity, similar to inverse piezoelectricity, manifests when a voltage is applied to the tip and moved away from its apex, resulting in a decaying electric field and an approximately radial electric field gradient. This electric field gradient induces a converse flexoelectric strain, which, when divided by the voltage applied to the tip, yields a nonzero effective piezoelectric coefficient in any dielectric material. Abdollahi *et al.*<sup>113</sup> theoretically and experimentally demonstrated that nonpiezoelectric SrTiO<sub>3</sub> dielectrics exhibit a significant effective piezoelectric coefficient due to inverse flexoelectricity. The magnitude of this gradient-induced apparent piezoelectricity decreases inversely with an increase in the force<sup>114,115</sup> between the AFM tip and the surface, as the tip and contact area experience an enlargement, resulting in a

reduction of the electric field gradient within the sample. In contrast, the pure piezoelectric response remains unaffected by external forces, enabling the distinction between inverse flexoelectric and conventional piezoelectric responses in the same material. Consequently, when we analyze the experimental data, it is important to note that under the indentation of the AFM tip, there are other effects that come into play in addition to the flexoelectric effect, such as piezoelectricity, Vegard strain effect, piezo-chemical effect, and triboelectricity, etc. Due to the complexity of measuring the strain gradient induced by the needle tip, it must be estimated based on an appropriate theoretical model.

Furthermore, the electric field and tip-induced strain gradients can induce variations in the local concentration of free ions within oxide films,<sup>109,116,117</sup> leading to localized volume expansion or contraction and resulting in piezoelectric-like deformations. Meanwhile, Fig. 9 illustrates the controlled manipulation of oxygen vacancy distribution through mechanical forces exerted by the PFM tip, indicating that strain gradients induced by the depolarization field enable the movement of oxygen vacancies.<sup>105</sup> By altering the tip geometry, spatial modulation of oxygen vacancies can be achieved, favoring the transverse transport of vacancies under the depolarization field. Furthermore, this modulation leads to abnormally high conductivity changes at domain walls and mixed-phase

boundaries.<sup>118,119</sup> Similarly, reversible switching between insulating and conducting states has been realized using the large strain gradient ( $\sim 10^7 \text{ m}^{-1}$ ) generated by pressing the AFM tip onto the ultrathin  $\text{SrTiO}_3$  surface.<sup>39</sup> The strain gradient induces the crossing of both the conduction band minimum and valence band maximum with the Fermi level. This energy band crossing reduces the width of the tunneling barrier while maintaining its height, resulting in a significant increase in tunneling conductance within the ultrathin dielectric and a substantial reduction in film resistivity. This approach harnesses the nondestructive application of strong electrostatic fields in various insulating systems by utilizing the purely mechanical force of the AFM/PFM tip as a dynamic tool. When an ultra-thin dielectric layer is polarized by a substantial strain gradient, the resulting depolarization field and electrostatic contributions not only modulate the distribution of oxygen vacancies,<sup>120–122</sup> but also significantly alter the tunnel barrier profile,<sup>56</sup> thereby triggering a quantum tunneling effect.

#### 4.2.2. From film bending deformation

Conventionally, strain engineering in oxide thin film growth is often limited by the rigid substrate and small lattice mismatches. These limitations impose constraints on the

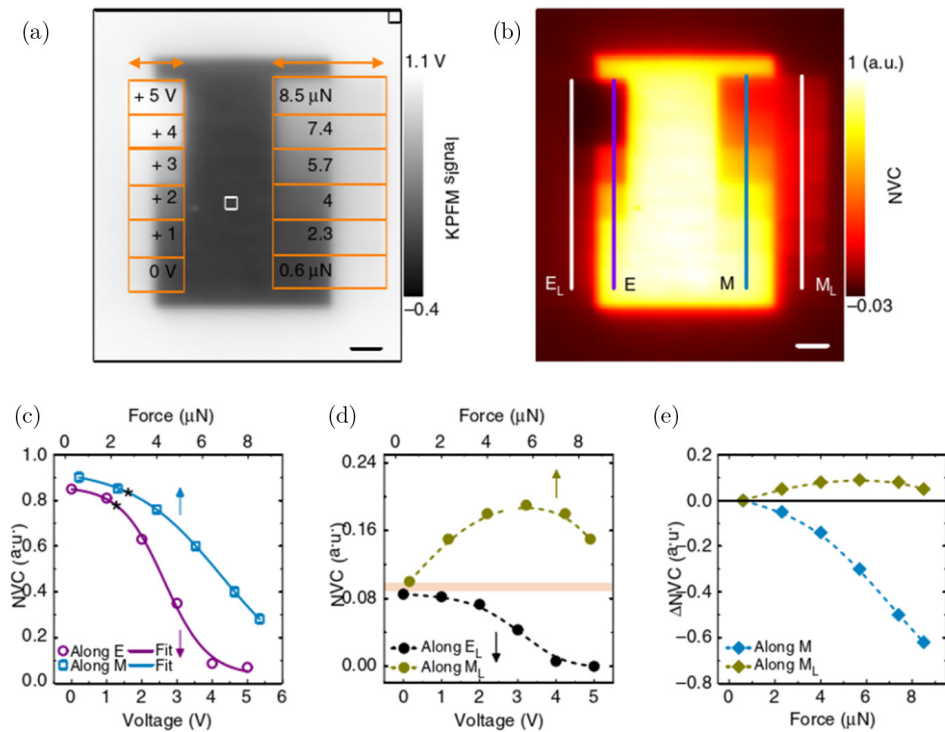


Fig. 9. (Color online) Characterization of oxygen vacancy redistribution by applied bias and force. (a) The KPFM image after electrical and mechanical scans were performed across borders between the  $V_o''$ -enriched and pristine regions. (b) The normalized vacancy concentration (NVC) map constructed from the KPFM image in (a). (c) The NVC along lines  $E$  (open circles) and  $M$  (open squares) in (b) measured as a function of applied bias and contact force, respectively. (d) The NVC along lines  $E_L$  (black-colored circles) and  $M_L$  (dark yellow-colored circles) in (b) measured as a function of applied bias and contact force, respectively. (e) Background-subtracted NVC ( $\Delta\text{NVC}$ ) along lines  $M$  (turquoise-colored diamonds) and  $M_L$  (dark yellow-colored diamonds) in (b).

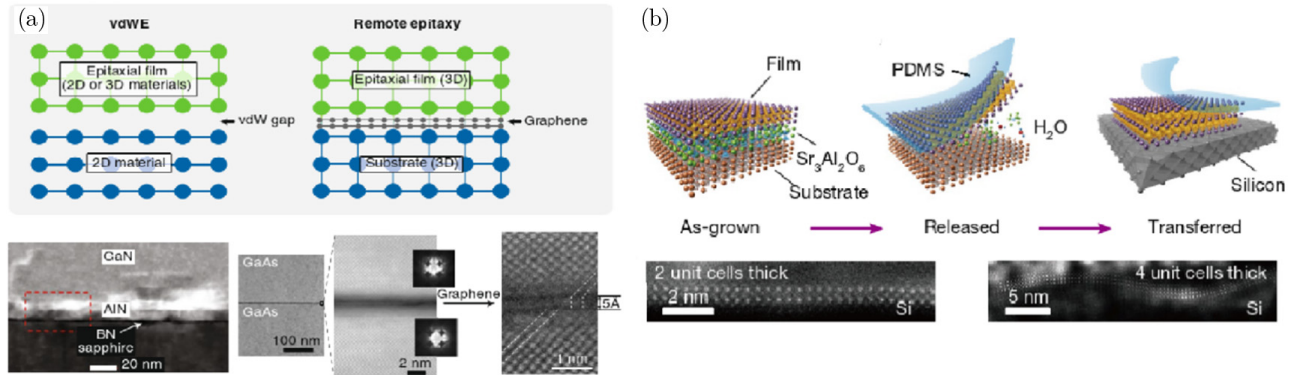


Fig. 10. Advanced epitaxy techniques, (a) illustration of epitaxy on 2D materials. For vdW, the epitaxial layer grows without any interaction with the host substrate (schematic, top left). The vdW layer becomes the seed for growth, which can be used to grow single-crystalline materials such as GaN as shown in the cross-sectional SEM image on the bottom left, in contrast, for remote epitaxy, a couple of monolayers of graphene are transferred or directly grown on the substrate and the epilayer is grown directly on top (schematic, top right). However, once the growth is finished, the epilayer can be exfoliated and transferred to any arbitrary substrate since the graphene acts as a sacrificial layer for exfoliation. An example of remote epitaxy of GaAs on GaAs is shown on the bottom right, showing cross-sectional SEM and TEM images of the GaAs/graphene/GaAs interface. (b) Growth and transfer of ultrathin freestanding SrTiO<sub>3</sub> films and atomically resolved cross-sectional of a two/four-unit-cell freestanding STO film transferred to a silicon wafer.

tunability and extensibility of strain and strain gradients due to factors such as fragile deformation and epitaxial conditions. However, the utilization of free-standing film systems offers a promising alternative. By stacking ultrathin layers (a few atoms thick) of 2D materials,<sup>123</sup> free-standing heterostructures can be achieved without restrictions on crystal structures. As shown in Fig. 10(a), the concept of transferring single materials or nanomaterial-based individual devices onto foreign substrates<sup>124–126</sup> showcases the versatility of this approach. In recent years, novel technologies such as lift-off and transfer have emerged,<sup>122</sup> enabling the fabrication of high-flexibility complex oxide nanofilms. For instance, the use of water-soluble Sr<sub>3</sub>Al<sub>2</sub>O<sub>6</sub> (SAO) as a sacrificial buffer material has provided a reliable method for synthesizing high-quality free-standing thin films.<sup>125</sup> This technique offers novel prospects for self-curved free-standing films, introducing an additional level of control to achieve sizable and adjustable strain gradients for enhancing the flexoelectric effect. Lun *et al.*<sup>127</sup> developed an electromechanical model to explore the flexoelectric effect in self-curved self-supported heterogeneous films. The study demonstrates that the effective flexoelectric polarizations are six times larger than the piezoelectric polarizations, and the manipulation of anisotropic interfacial mismatch strain and release direction by adjusting the ratio of interfacial mismatch strain, film thickness, and film-base thickness enables the formation of self-curved morphologies (such as ring, spring, and twisted ribbon) with different flexoelectric polarizations. These unconventional low-dimensional systems hold the potential for inducing unique physical and mechanical responses through electromechanical coupling effects, opening new avenues for research.

The remarkable flexibility of these oxide materials<sup>128</sup> allows for the generation of substantial strain gradients

reaching  $\sim 10^{-7} \text{ m}^{-1}$  during the bending process,<sup>129</sup> owing to the ultrathin nature of the films. Nanoscale mechanical bending offers novel physical phenomena driven by larger flexoelectricity, such as modulated electrical transport,<sup>62</sup> enhanced photovoltaic effect,<sup>130</sup> strain gradient-dependent resistivity,<sup>106</sup> etc. Ji *et al.*<sup>131</sup> successfully prepared free-standing thin films of composite oxides (e.g., SrTiO<sub>3</sub>, BiFeO<sub>3</sub>) with thicknesses almost down to monolayer, and demonstrated for the first time that they can be synthesized and transferred to any desired substrate, as shown in Fig. 10(b). The bending state of self-supporting films of BFO and STO films ( $\sim 5 \text{ nm}$  thick) with wrinkles leads to strain gradients up to  $3.5 \times 10^7 \text{ m}^{-1}$ .<sup>129</sup> These curved self-supporting perovskite oxides demonstrate enhanced polarization, enabling the modulation of charge carrier transport properties. The source of the enhanced polarization is primarily derived from the flexoelectrical response induced by the strain gradient. By simply bending the transferred free-standing films on flexible substrates, they were able to achieve continuously adjustable strain gradients in large-area films.<sup>132</sup> These controllable strain gradients induce additional electric fields through the flexoelectric effect, which, combined with the built-in electric field, enable tunable photoconductivity in the free-standing BiFeO<sub>3</sub> thin films. This tunability allows for electrical/mechanical writing and optical readout. By utilizing the strain gradient as an additional degree of freedom, the physical properties of the films can be tailored for flexible electronics. Furthermore, polymers have several advantages that make them more convenient in bending applications. In addition to this, it is often used as a carrier for nanoxide films. At the same time, they are more flexible and brittle, and when stresses reach a certain level, the high strain gradients required to produce a significant flexoelectric effect can be achieved while avoiding catastrophic damage. Zhang *et al.*<sup>133</sup> investigated the high flexoelectric effect of porous



polymeric materials by theoretical modeling. They pointed out that compared with solid materials, porous materials can exhibit flexoelectric properties in arbitrary loading forms with much higher specific flexoelectric outputs due to their complex microstructures. Taking inspiration from this finding, Ruiz *et al.*<sup>134</sup> employed solution blow spinning (SBS) technique to fabricate multilayers of nanoparticle-doped PVDF filled with multi-walled carbon nanotubes. The flexoelectric behavior of poly(vinylidene fluoride) was examined, and it was observed that the inclusion of nanoparticles facilitated the formation of polarized nanodomains following strain, thereby enhancing the flexoelectric effect. This study provides valuable insights into exploring the flexoelectric behavior of polymer-oxide films and designing PVDF-based materials with enhanced flexoelectric yields.

Van der Waals heteroepitaxy was initially developed as a method to demonstrate the epitaxial growth of 2D layered materials on other 2D layered materials.<sup>124,135,136</sup> This approach has now been extended to include the epitaxial growth of functional oxides on 2D materials. For example, Chu's group succeeded in preparing various oxide films on layered mica substrates<sup>137–139</sup> Importantly, the flexible and easily foldable nature of 2D layered materials enables the investigation of strain effects on the physical properties of transition metal oxides. Remarkable progress has been made in this field, such as the uniaxial strain modulation of

heterostructures comprising  $\text{La}_{0.67}\text{Sr}_{0.33}\text{MnO}_3$  (LSMO) and BTO films,<sup>140</sup> reducing threshold of domain switching in 2D ferroelectrics via electrical–mechanical coupling,<sup>141</sup> and defect engineering of self-supporting single-crystal nanofilm heterostructures,<sup>142–144</sup> etc. These advancements serve as inspiration for future extensive research on flexoelectricity, as these 2D films can withstand unprecedentedly large strains and strain gradients, leading to the emergence of exotic electromechanical coupling phenomena.

Large deformations induced by bending can produce significant strain gradients that naturally break inversion symmetry in thin-film materials. This breaking of inversion symmetry results in modifications to the electron ground state,<sup>145,146</sup> leading to intriguing electrical transport properties such as superconductivity and charge-spin jumps. Notably, the impact of inversion asymmetry on energy bands is particularly pronounced in transition metal oxides with strong spin-orbit coupling.<sup>147,148</sup> Moreover, oxide films also demonstrate superelasticity and superflexibility when subjected to extreme bending deformations, as illustrated in Fig. 11. Superelasticity arises from the dynamic evolution of ferroelectric nanodomains, where dipoles continuously rotate among different nanodomains,<sup>125</sup> creating a continuous transition zone capable of accommodating varying strains. It is worth noting that flexoelectricity is predicted to be very large for thin film materials under bending deformation,

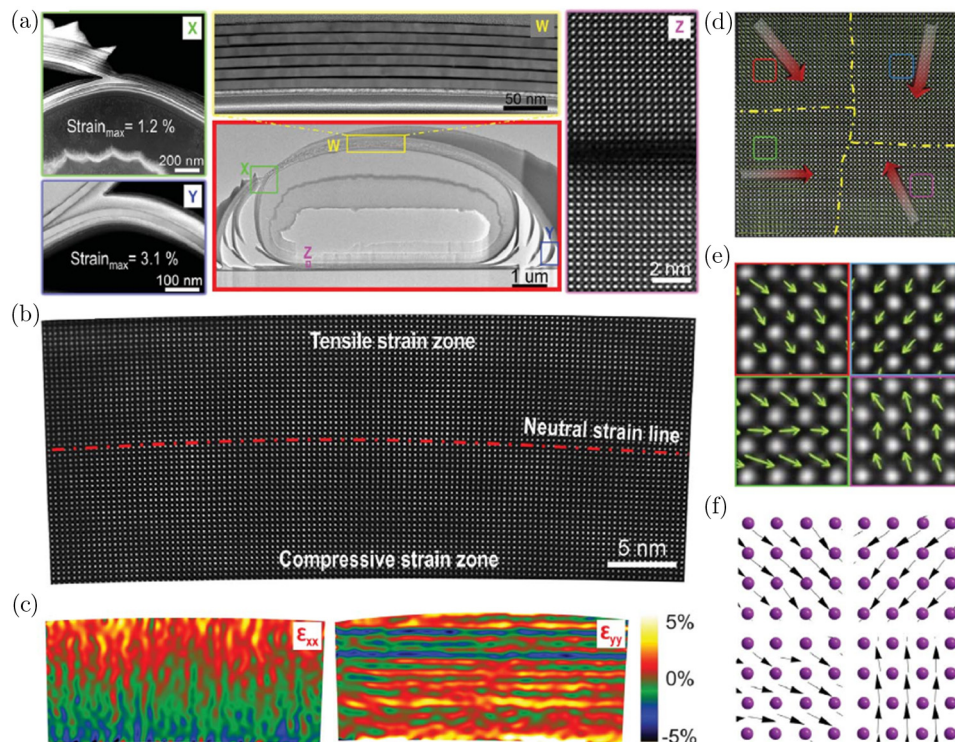


Fig. 11. Atomic-scale spatial distribution of continuous and curved lattice. (a) Cross-sectional STEM and TEM images of multilayer BTO roll with magnified images of the different regions. (b), (c) Atomic-scale STEM and geometric phase analysis images of BTO. (d) Atomic-scale STEM together with Ti displacement of the region with strain max  $\sim 3.1\%$ . (e) Magnified images of the four regions from (d). Dipole displacements are amplified by a factor of 15 for clarity. (f) The dipole configurations in four selected areas of a bent membrane by atomistic simulations.



however, flexoelectric bending consistent with current theoretical work, i.e., strains comparable to or greater than the yield strains of typical materials, has not been directly observed, and it remains to be verified whether such large effects are physically real, or merely a nominal extrapolation. Recently, Koirala *et al.*<sup>149</sup> employed transmission electron microscopy (TEM) to directly observe large-scale reversible bending at the nanoscale driven by the inverse flexoelectric effect. Thin features exhibited bending angles of up to 90° with curvature radii of approximately 1 μm, corresponding to substantial nominal strains. This experimental evidence validates the occurrence of significant flexoelectric bending at the nanoscale and establishes a basis for further investigations in this area.

The development of advanced flexible ferroelectric electronics necessitates the utilization of flexible ferroelectric films to meet the growing demand for applications.<sup>150,151</sup> 2D oxide thin films offer a viable platform for designing high-performance nanoelectromechanical systems (NEMS). Wang *et al.*<sup>152</sup> pioneered using AFM tips to bend ZnO nanowires to construct piezoelectric nanogenerators (PENGs), accompanied by flexoelectric effects. However, the vast majority of nanogenerators under stress are currently PENG, while flexoelectricity is still in its infancy, and there has been little work on pure flexoelectric nanogenerators (FENGs).<sup>107</sup> Unfortunately, conventional nanogenerators face technical limitations as they can only produce transient pulsed electrical signals,<sup>153–156</sup> and achieving long-term continuous output remains challenging. Essentially, nanogenerators deform the crystal lattice through external forces, thereby inducing polarization and dipoles in the crystal. The objective is to maximize the directional movement of carriers driven by the polarization potential (work); however, it is challenging to deposit electrodes along the radial direction, especially in dense 1D nanowire arrays. Consequently, obtaining piezoelectric/flexoelectric output from the *c*-axis direction proves to be difficult. Building upon these findings, Li *et al.*<sup>157</sup> proposed and fabricated a novel approach for the controlled growth of 2D FENGs single crystals. By subjecting the thin-film FENGs to asymmetric bending, a directional built-in polarization potential aligned with the output electric field was achieved. This development marks the first instance of continuous and stable voltage and current signals being generated by nanogenerators. Additionally, the widespread presence of flexoelectricity enables the simplified design of flexoelectric NEMS devices with enhanced thermal stability,<sup>158</sup> thereby expanding the scope of research and potential applications for nanogenerators.

## 5. Other Physical Phenomena Coupled with Flexoelectric Effect in Thin Film

### 5.1. Flexomagnetic effect

The flexomagnetic effect (FIM) is the strain gradient-induced magnetization, which is derived from the strain gradient

magnetic effect in addition to the strain (piezomagnetic effect) and quadratic (second-order magnetoelastic effect) in the net magnetization of the system in Eq. (3).<sup>52</sup> By taking partial derivative of free energy (proportional to the product of the magnetic field component  $H_i$  and the conjugate terms involving mechanical strain) with respect to magnetic field component, we get the net magnetization in the system. Although, for calculated values of strain gradient, the contribution of the flexomagnetic effect to magnetization is smaller than that of the nonlinear magnetoelastic effect. The relative contribution of the flexomagnetic effect is increasing with the decreasing strain gradient due to its linear nature and dependence on strain gradient while the nonlinear magnetoelastic effect is quadratic in its lowest power.

$$M_i = \underbrace{\lambda_{i,jk}\sigma_{jk}}_{\text{piezo}} + \underbrace{\mu_{i,jk}\sigma_{jk}^2}_{\text{mag-elast}} + \underbrace{v_{ijkl}E \frac{\partial \varepsilon_{jk}}{\partial x_l}}_{\text{flexo}}; \quad i, j, k, l = 1, 2, 3, \quad (3)$$

where  $\lambda_{i,jk}$  is the piezomagnetic tensor,  $H_i$  is the *i*th component of the magnetic field,  $\sigma_{jk}$  is the elastic stress tensor,  $\mu_{i,jk}$  is the magnetoelastic tensor,  $v_{ijkl}$  is the four-rank tensor (flexomagnetic tensor),  $\partial \varepsilon_{jk} / \partial x_l$  is the strain gradient and  $E$  is the elastic modulus. The dummy indices “*ijk*” are independent of each other,<sup>159</sup> it uses the Einstein summation convention to  $M_i$ .

In contrast to the flexoelectric effect, where electrical polarization is directly related to atomic displacement, the flexomagnetic effect is indirect. It occurs due to spin-exchange interactions that cause the atomic spins to reorient after atomic displacement. The flexomagnetic effect is linear and caused by the strain’s inhomogeneity, as shown in Figs. 12(a) and 12(b). Therefore, there is no flexomagnetic effect in the ground state or the case of external uniform strain. The main mechanism behind flexomagnetic is that spin-exchange interactions depend on interatomic distances. When a strain gradient is applied, the distance becomes unequal, resulting in out-of-plane rotations of the local magnetic moments. Due to these rotations, the system acquires a nonzero net magnetic moment.<sup>160</sup> Due to surface and size effects, the inherent inhomogeneity of order parameters in ferroic nanosystems can induce mechanical strain-spontaneous flexocoupling or flexomagnetic effects,<sup>21</sup> causing changes in the properties of ferroic nanostructures.

The advancement of piezoelectric force microscope (PFM) techniques has enabled direct observation of ferroelectric domains, swift ferroelectric domains, and magnetic domains.<sup>161,162</sup> as shown in Fig. 12(c). This breakthrough has facilitated the direct visualization of the coupling between magnetic and ferroelectric domains, providing a powerful tool for magnetoelectric research. In multiferroic Bi<sub>5</sub>Ti<sub>3</sub>FeO<sub>15</sub> thin films, the regulation of ferroelectric domains and magnetic domains is achieved through the application of electric fields and external mechanical forces. Under the sole application of an electric field, the nanoscale mixed phase region’s magnetic

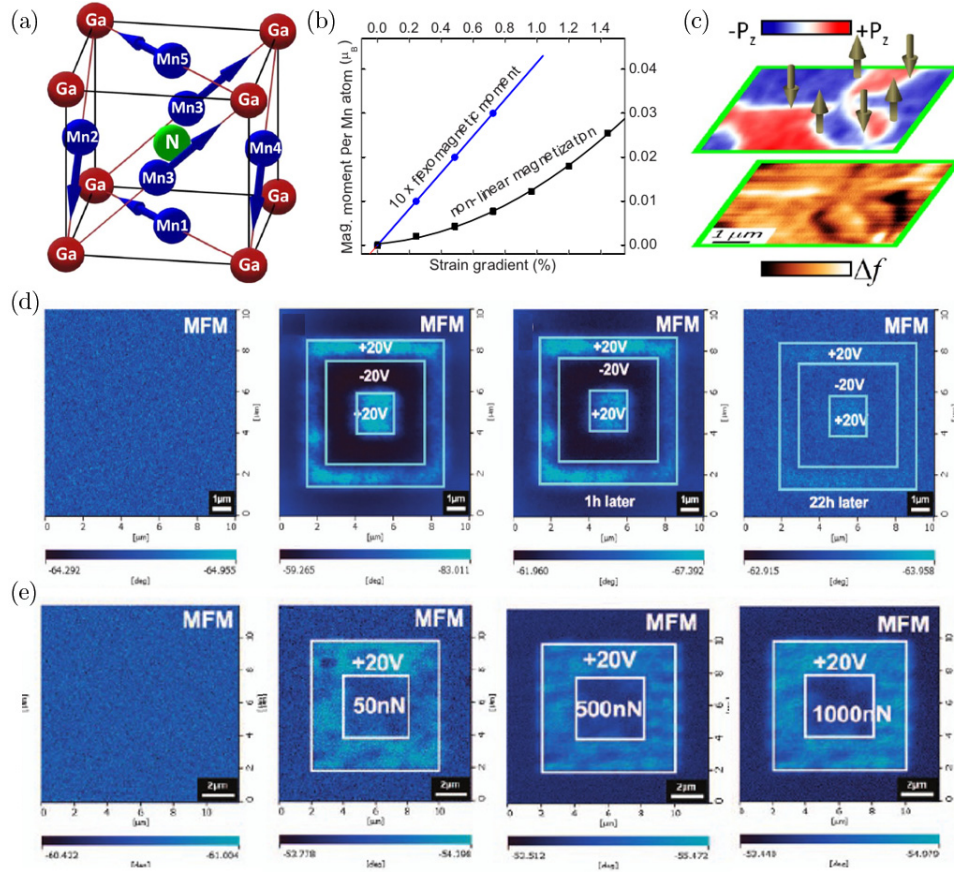


Fig. 12. (Color online) (a) Ground state of the antiperovskite  $\text{Mn}_3\text{GaN}$  unit cell: noncollinear  $\Gamma^{5g}$  magnetic structure. Local magnetic moments are shown by blue arrow on Mn atoms. (b) Linear out-of-plane ( $\times 10$ ) (blue circles) and nonlinear in-plane (black squares) induced net magnetization of Mn atom as a function of the strain gradient. (c) A perspective view of PFM and magnetic force microscopy (MFM) images with arrows representing the orientation of the uncompensated magnetic moments at structural antiphase-ferroelectric Domain Walls (DWs). (d) MFM image poled by  $+20\text{V}$  in the area of  $7 \times 7 \mu\text{m}^2$ ,  $-20\text{V}$  in  $5 \times 5 \mu\text{m}^2$  and  $+20\text{V}$  in  $2 \times 2 \mu\text{m}^2$ , with reading over  $10 \times 10 \mu\text{m}^2$  and evolution of MFM images of the poled BTF thin film collected after removing the electric field. MFM images before and after electric and mechanical switching. (e) The  $\text{Bi}_5\text{FeTi}_3\text{O}_{15}$  (BTF) thin film that was first poled by positive electric bias of  $+20\text{V}$  over  $8 \times 8 \mu\text{m}^2$ , and then switched by mechanical forces of 50, 500, 1000 nN in the center over  $4 \times 4 \mu\text{m}^2$ , respectively.

moment can be erased and rewritten at room temperature via the electric field modulation of the magnetic force,<sup>163</sup> as depicted in Figs. 12(d) and 12(e). Simultaneously, when a mechanical force is exclusively exerted by the AFM tip, it effectively drives a transition in the local ferroelastic strain state. This leads to a reversal of polarization and magnetization in a manner reminiscent of an electric field,<sup>161</sup> providing confirmation of magnetic and magnetoelectric coupling in the thin film. Similarly to flexoelectric coupling, the flexomagnetic effect is anticipated to play a vital role in the domain structures and their dynamics and thermodynamics at the micro- and nanoscale. This effect is particularly relevant in systems such as nonferromagnetic or antiferromagnetic thin films, nanoparticles, magnetic vortices, and skyrmions. For instance, Naimov<sup>164</sup> introduced the concept of flexomagnetic coupling to analyze the influence of nonuniform strain on the energy band structure of graphene. Ling *et al.*<sup>165</sup> demonstrate that the nonuniform gradients of external strain (flexomagnetic

effect) can induce the partial structural phase transition from FCC to BCC in the wrinkled high-entropy alloy (HEA) thin film. Spurgeon *et al.*<sup>166</sup> experimentally studied magnetoelectric oxide heterostructures, commonly used in spintronics, and observed local structural distortion and interface shielding of ferroelectrically bonded surface charges, resulting in a graded magnetization phenomenon due to flexomagnetic coupling. Additionally, Ghobadi *et al.*<sup>167</sup> incorporated flexomagnetic coupling into the phenomenological analysis of nanoplates subjected to magnetic flux. These studies collectively underscore the significance of flexomagnetic coupling in various systems and lay the foundation for further exploration in this field.

The flexomagnetoelectric effect is a phenomenon that links the magnetic and electric order parameters through their gradients.<sup>168</sup> This effect can be induced by either strain gradients (known as direct flexoelectric or flexomagnetic effects) or magnetization gradients (known as inverse flexomagnetic

effects), resulting in the absence of spatial inversion symmetry. Consequently, a specific magnetic order with a noncollinear magnetic structure arises, leading to the emergence of electric polarization. Although most magnetoelectric materials exhibit small magnetoelectric effects, some new multiferroics with giant magnetoelectric effects<sup>169</sup> have been found to break this limitation. Moreover, even weak magnetoelectric interactions can produce remarkable cross-coupling effects<sup>170</sup> when electric polarization is induced in a magnetically ordered state. Zvezdin and Pyatakov<sup>168</sup> investigated the nonuniform magnetoelectric interactions in bismuth ferrite. They found that inhomogeneous magnetoelectric interactions can induce spin modulation, thereby enhancing electrical polarization. This modulation occurs as a result of flexomagnetolectric interactions, which are induced by manipulating the spatial distribution of magnetization strength in multiferroics. The flexomagnetic effects in nanostructures are strongly influenced by the strain gradient and magnetic field. Previous researches<sup>171–173</sup> have emphasized that the importance of flexomagnetic effect becomes increasingly prominent at the nanoscale, despite its relatively weaker manifestation compared to the piezomagnetic effect at the macroscopic scale. Malikan *et al.*<sup>174,175</sup> conducted studies on the size-dependent thermal stability of micro- and nanobeams, considering the functionally graded piezomagnetic and converse flexomagnetic effects under temperature distributions. In a recent study, Momeni-Khabisi and Tahani<sup>176</sup> examined the linear and nonlinear buckling behavior of piezo-flexomagnetic nanoplate strips, considering geometrical imperfections. They derived the size-dependent governing equations and associated boundary conditions for the system. In addition, nanostructures may be unconsciously in contact with external magnetic fields, which can have an effect on their properties. In order to reduce the errors and to design rationally, it is necessary to study the influence of flexomagnetic effects on the mechanical behavior of nanostructures. Momeni-Khabisi<sup>177</sup> conducted a study focusing on the analytical formulations and solution procedures for the thermal stability properties of piezomagnetic nanosensors and nanoactuators, considering the influence of flexomagnetic effects and geometrical imperfections. The study proposed closed-form solutions and presented numerical results, which can serve as valuable benchmarks for future piezoflexomagnetic nanosensors and nanoactuators analyses.

## 5.2. Flexophotovoltaic effect

Discovery of the photovoltaic effect in perovskites and ferroelectric oxides<sup>178,179</sup> has opened up promising opportunities for their application in photovoltaics. Conventional solar cells face a significant limitation in achieving high open-circuit voltage ( $V_{oc}$ ) due to the relatively large Schottky barrier height (SBH). In contrast, the ferroelectric photovoltaic effect has a large open-circuit voltage above the bandgap,<sup>55</sup> which means that the carrier separation mechanism

driven by ferroelectric polarization is fundamentally different from that of conventional semiconductor p–n junctions. Photogenerated carrier transport in ferroelectrics is strongly influenced by their spontaneous polarization, which generates an electric field much stronger than the built-in electric field in heterojunctions, leading to a notably enhanced photoresponse. To date, extensive research has been conducted on various ferroelectric materials<sup>180–182</sup> such as  $\text{Pb}(\text{Zr,Ti})\text{O}_3$ , BTO, and  $\text{BiFeO}_3$ . These materials have been successfully fabricated into photovoltaic modules and employed for efficient solar energy harvesting. This underscores the considerable potential of ferroelectric oxides in advancing the field of photovoltaics. Manipulation of physical properties through flexoelectric polarization has been observed in semiconductors, transition metal oxides, and perovskite oxides. For example, polarization-enhanced photocatalysis,<sup>183,184</sup> energy storage,<sup>185</sup> flexible electronics,<sup>186</sup> fatigue-free ferroelectric memory,<sup>187</sup> topotactic phase transformation,<sup>188</sup> flexophotocatalysis,<sup>189</sup> etc. Yang *et al.*<sup>12</sup> used an AFM tip to introduce a strain gradient in the tip-surface contact region to generate a stable photovoltaic current in the center-symmetrical single-crystal  $\text{SrTiO}_3$  and  $\text{TiO}_2$ . This photovoltaic effect induced by strain gradient is called the FPV effect. Due to the gradient strain-induced breaking of inversion symmetry, a polarization field with a preferred orientation is generated. The variation of electric field caused by the strain gradient leads to the formation of a gradient electric potential within the material. Under illumination, this gradient electric potential induces the separation and motion of photo-excited charge carriers in the material. As a result, electrons and holes are separated and driven to different regions, resulting in charge separation. Although some scholars<sup>190</sup> pointed out that the experimental results are not enough to verify the FPV mechanism, and raised several questions related to the experimental results, such as the rationality of the experimental design, physical model, calculation and analysis, etc., however, due to this effect, it is expected to overcome the thermodynamic Shockley–Queisser limit of conventional p–n junction solar cells, which extends the existing solar cell technology.

When materials are scaled down to the nanometer range since the size of the strain gradient is inversely proportional to its relaxation length, the flexoelectric effects will be significantly enhanced,<sup>93</sup> and conductive AFM (CAFM) probes coated with metal can introduce strain gradients and simultaneously monitor the current flow through the junctions. Accordingly, Pu *et al.*<sup>191</sup> proposed an electromechanical approach to enhance photovoltaic efficiency based on the flexoelectric effect. Figures 13(a) and 13(b) illustrate the experimental setup where an CAFM tip applies a force in the heterojunction to generate a strain gradient. *In-situ* current measurements were carried out, and a current–voltage ( $I$ – $V$ ) response under the strain gradient was obtained. Notably, the photovoltaic performance exhibited a significant improvement, with a  $V_{oc}$  increase of up to 20%, leading to a notable



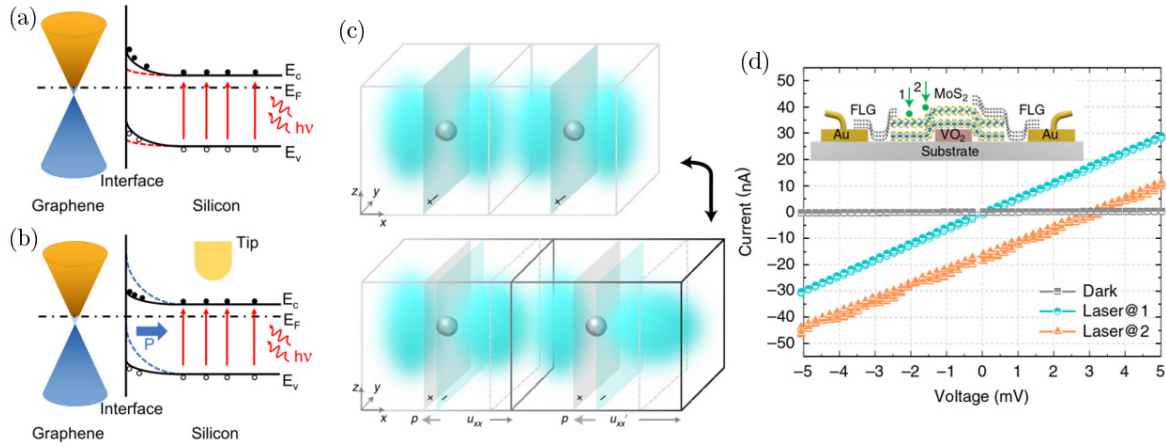


Fig. 13. (Color online) (a) Energy bandgap structure of the GSJ with laser on. (b) The bandgap structure bending by tip-pressing induced flexoelectricity modulation. (c) Electron cloud ( $p_x$  orbitals) distributions without (upper panel) and with (bottom panel) a strain gradient (strains  $u_{xx}$  and  $u'_{xx}$ , gray arrows). Electron redistribution shifts the negative charge center (on the light cyan plane) away from the positive charge center (on the light gray plane) along  $x$ , leading to a negative dipole moment  $p$  (bold gray arrow) in each unit cell. (d) FPV effect of the MoS<sub>2</sub> sheet at room temperature, current-voltage curves of the device under laser (532 nm) illumination at spot 1 (Laser@1) and 2 (Laser@2) and without illumination (Dark). The inset shows a schematic of the cross-sectional view of the device.

enhancement in power conversion efficiency. The flexoelectric effect offers a means to tune the barrier height of Schottky junction interfaces,<sup>183,192</sup> and the FPV effect was observed in perovskite films, demonstrating a remarkable enhancement in solar cell performance.

Considering that the lattice distortion and crystallographic disorder at the interface in epitaxial films also can generate large strain gradients, potential research opportunities can be opened for the FPV effect. Due to the inhomogeneous lattice distortion, a considerable strain gradient is generated, and an additional effective built-in electric field is generated by the flexoelectric effect, which can simultaneously generate pyroelectric current and photovoltaic current during the illumination process.<sup>193</sup> Guo *et al.*<sup>132</sup> investigated the tunable photovoltaic behavior in self-supporting BiFeO<sub>3</sub> films, wherein the autonomous bending of the flexible substrate induced nonuniform lattice distortions and continuous strain gradients. The increase/decrease of photocurrent is achieved through the coupling between the unidirectional strain gradients induced by the convex bending and the ferroelectric polarization switching. By engineering strain gradients in the dielectric layer, Jiang *et al.*<sup>194</sup> achieved bidirectional tunability of the FPV behavior in LFO/LNO/LAO epitaxial thin-film heterostructures. This was achieved by employing the concave/convex bending of mica substrates, with the LAO layer serving as the stretching layer to apply compressive stress to the LFO layer due to its smaller lattice constant. The resulting strain gradient, reaching approximately  $10^6 \text{ m}^{-1}$ , was accompanied by flexoelectric polarization modulation of the band alignment, leading to a remarkable photovoltaic effect with a short-circuit current density of  $\sim 0.4 \text{ mA/cm}^2$ .

Furthermore, the exploration of strain gradient engineering to induce FPV effects in 2D material systems<sup>16,195</sup> has addressed a critical gap in this research field.

The polarization field plays a significant role in the separation of photogenerated electron-hole pairs. By coupling strain gradient-induced flexoelectric polarization with semiconductor properties, electronic/photon-electronic phenomena such as giant flexoelectric effect,<sup>196</sup> FPV effect,<sup>16,195,197</sup> photo-flexoelectric effect,<sup>13,198,199</sup> and flexoelectronics,<sup>183,200</sup> etc. can be achieved. The presence of large strains in 2D materials offers the possibility of exploring potential giant strain gradient effects. Additionally, during the growth process of 2D materials, various bending structures such as nanotubes, curls, ripples, and bubbles are easily formed. These bent structures under nonuniform mechanical conditions can exhibit significant flexoelectric effects and induce rich physical phenomena. They can be utilized to control properties such as conductivity, Fermi level movement, and direct-indirect bandgap transition in 2D materials.<sup>201</sup> For instance, incorporating lattice curvature and magnetic doping in monolayer MoS<sub>2</sub> has been predicted to exhibit a significant flexoelectric magnetoelectric effect.<sup>202</sup> Quantum-like pseudo-magnetic fields emerge in curved graphene ribbons, resulting in Landau levels.<sup>203</sup> Folded monolayers of MoS<sub>2</sub> exhibit giant band tuning effects.<sup>204</sup> The conventional understanding of the flexoelectric effect suggests that lattice contributions arise from internal atomic displacements. Consequently, the micro-mechanisms of the flexoelectric effect often employ the concept of ions responding to strain gradients to induce polarization. From a microscopic standpoint, the flexoelectric effect encompasses two types of contributions: the lattice contribution attributed to internal atomic displacements based on the rigid ion model,<sup>93</sup> and the electronic contribution associated with atomic displacements leading to charge density redistribution,<sup>205</sup> as shown in Fig. 13(c). However, this conventional viewpoint tends to overlook the more fundamental role played by electronic distribution in the microscopic mechanism of flexoelectricity.



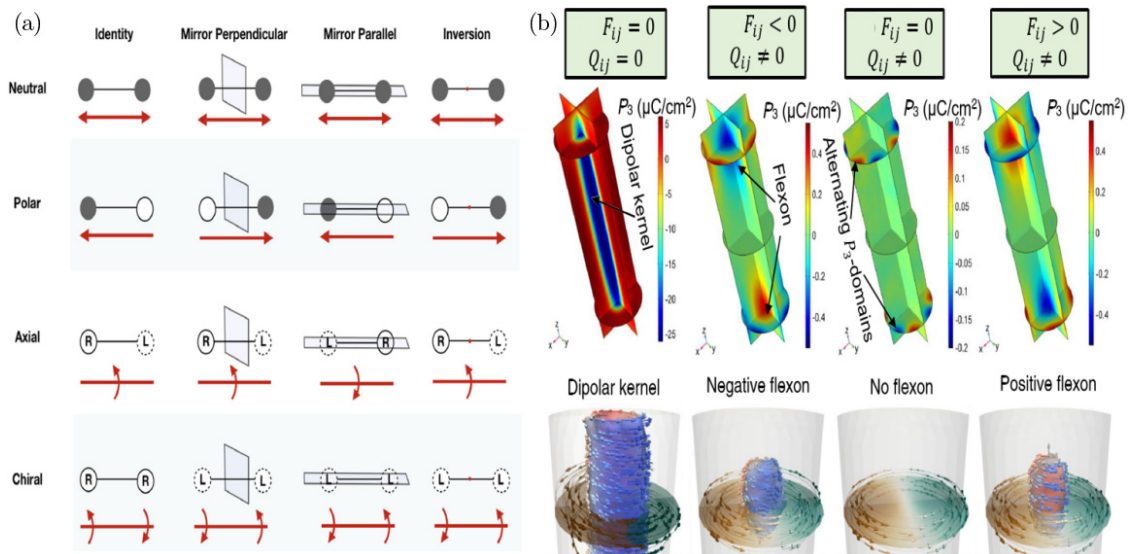


Fig. 14. (a) Transformation properties of four possible time-invariant dipoles, each row corresponds to one of the dipoles. The first column indicates the name of the dipole property in the row, each subsequent column indicates the effect of one selected isometry operation on these dipoles, which is either an invariance or a sign reversal. (b) Distribution of the polarization component  $P_3$  (top row) inside a cylindrical nanoparticle and a magnified view on the flexon-structure (bottom row). The arrows show the orientation of polarization vector  $P$ . The images are calculated without electrostriction ( $Q_{ij} = 0$ ) and flexoelectric ( $F_{ij} = 0$ ) couplings; with electrostriction coupling ( $Q_{ij} \neq 0$ ) and negative, or zero, or positive values of flexoelectric coefficients  $F_{ij}$ .

In this context, Jiang *et al.*<sup>16</sup> propose a unique strategy to generate and modulate strain gradients in 2D materials, achieving enhanced flexoelectric inversion symmetry and the existence of extraordinary photovoltaic effects in 2D materials. As shown in Fig. 13(d), it is based on a strain gradient engineering approach to the structural inhomogeneity and phase transition of a hybrid system composed of MoS<sub>2</sub> and VO<sub>2</sub>. At the interface between phase-change and nonphase-change materials, strain gradients are anticipated to emerge, influencing the electronic density distribution and giving rise to a nonzero dipole moment (i.e., flexoelectricity) along the direction of the strain gradient. Experimental observations reveal that the photovoltaic coefficient of MoS<sub>2</sub> is several orders of magnitude higher than that of most noncentro-symmetric materials, thereby presenting an avenue for exploring the FPV effect in 2D materials. These discoveries advance our fundamental comprehension of the FPV effect and open up new possibilities in terms of theoretical concepts and potential materials for photovoltaic applications.

### 5.3. Chiral polarization textures

In studying ferroelectric material systems, the formation of ferroelectric domain structures is a central aspect and more generally the micron and nanoscale structures of polarization fields.<sup>206</sup> In ferroelectric thin films and nanoparticles, polarized structures are strongly influenced by electrostatic (depolarizing) fields<sup>99,207,208</sup> as well as by strain and strain gradients<sup>209,210</sup> via flexoelectric effects,<sup>28,211</sup> providing a flexible stage for polar chiral structure studies. Similar to the

Dzyaloshinskii–Moriya Interaction (DMI) postulated in the classical magnetic Bloch–Moriya theory of stable chiral ferromagnets,<sup>212,213</sup> scientists in ferroelectric research wanted to replicate the success of chiral structures in magnetic properties, explored the possibility of “ferroelectric DMI” and predicted the existence of ferroelectric counterparts of DMI by first-principle simulations.<sup>214</sup> Recently, Erb and Hlinka<sup>215</sup> deduced the possibility of identifying the orientational domain state of the asymmetric phase by using the “vector” physics knowledge of polar axial, chiral, and neutral dipole through computer algorithms (as shown in Fig. 14(a)), and they concluded that ferroelectric DMI could exist.

Furthermore, Morozovska *et al.*<sup>216</sup> presented a theoretical study of the ferroelectricity polar textures in cylindrical core–shell nanoparticles based on the phenomenological LGD method and finite element simulations. The calculations reveal a chiral polarization structure containing two oppositely oriented diffuse axial domains located near the cylinder ends, separated by a region with a zero-axial polarization and can be switched by reversing the sign of the flexoelectric coefficient as shown in Fig. 14(b). This finding suggests that DMI in ferroelectrics is not the only possible mechanism for forming homochiral polarization states and that anisotropic flexoelectric effects provide another way to stabilize such structures in ferroelectric nanostructures.

## 6. Conclusion and Outlook

Nanoscale flexoelectricity in oxide thin films is an emerging research area that holds immense promise for future practical

device applications, owing to their remarkable material suitability. The primary focus of current research within this field is to delve deeper into the understanding of the flexoelectric effect and its underlying mechanisms. Furthermore, several research groups are devoted to exploring the application of flexoelectric devices and enhancing their performance parameters. This review encompasses the experimental advancements made in studying flexoelectric effects, while briefly discussing their pertinent properties. Initially, the various sources of nanoscale flexoelectric effects are addressed, and three key characteristics of flexoelectricity are highlighted. First, it is universally observed in dielectric materials, disregarding their symmetry or chemical composition. This characteristic has sparked significant scientific interest, as flexoelectricity does not rely on specific material classes or device environments. Second, as the size of the material is reduced to the nanoscale, the magnitude of the induced flexoelectric field becomes notable, thereby modifying the physical properties of the material. Lastly, strain gradients in thin-film materials naturally break the inversion symmetry, thus resulting in alterations to the electron ground state and affecting peculiar structures and properties.





In recent years, remarkable progress has been achieved in thin film fabrication techniques and theoretical approaches, enabling the synthesis of diverse complex structure hetero-junction oxide films. Concurrently, significant advancements have also been made in investigating the generation and mechanism of nanoscale flexoelectricity, leveraging methods such as lattice mismatch and PFM/AFM tip pressing. Due to the weak van der Waals force bonding at part of the interface, the clamping effect from the substrate is eliminated, the film glides over the surface without stretching or compressing and the intrinsic flexoelectric coefficient can be measured. However, when conducting AFM-based experiments, it is crucial to consider the coexistence of piezoelectricity and flexoelectricity, as they can potentially contribute to the observed experimental results. Therefore, it becomes imperative to discern between the effects resulting from strain gradients and other factors, necessitating the development of specific methodologies to address this challenge. Inversion symmetry breaking in materials with strong spin-orbit coupling can yield spin-band splitting, resulting in the emergence of exotic electronic states and novel spintronic functionalities. Localized inversion symmetry breaking induced by AFM tip indentation provides a platform to study the flexophotovoltaic effect and the generation of magnetic skyrmions in centrosymmetric materials. By exploiting the mutual coupling between the photovoltaic effect and the flexoelectric effect, the enhancement of photovoltaic current is achieved, while the flexoelectric coefficient is significantly enhanced by several orders of magnitude under the combined stimulation of light and mechanical vibration. The exploration of strain gradient engineering to induce FPV effects in 2D material systems extends the application of photovoltaic effects.

Despite significant advancements in flexoelectricity research, many of the observed flexoelectric effects remain inadequately understood, necessitating ongoing research efforts and the formulation of comprehensive theoretical frameworks. For example, the understanding of flexoelectricity in crystalline is yet to be fully elucidated. Moreover, the achievement of tunable flexoelectric behavior in specific thin films remains an ongoing challenge. Although three direct measurement methods have been recently developed for quantifying the transverse, longitudinal, and shear flexoelectric coefficients, the fundamental issue of accurately measuring the flexoelectric coefficient of thin film materials remains unresolved. The sensitivity of flexoelectric effects to the local environment underscores the pressing need for advancements in characterization techniques to precisely assess the local strain state of thin films and thereby reliably determine the flexoelectric coefficients. Furthermore, the relationship between surface flexoelectricity and surface piezoelectricity remains unclear, necessitating further investigation, the utilization, and development of FPV devices all need to be explored in depth.

### Acknowledgments

This work was supported by the National Natural Science Foundation of China (Nos. 51962020, 12174174). Support from the Natural Science Foundation of Jiangxi Province (No. 20212ACB214011) was also acknowledged.

### ORCID

Guoyang Shen  <https://orcid.org/0009-0009-9766-4295>  
 Renhong Liang  <https://orcid.org/0009-0003-5330-1691>  
 Zhiguo Wang  <https://orcid.org/0000-0001-9409-1334>  
 Longlong Shu  <https://orcid.org/0000-0002-7121-1652>

### References

- <sup>1</sup>B. Chu, W. Zhu, N. Li and L. Eric Cross, Flexure mode flexoelectric piezoelectric composites, *J. Appl. Phys.* **106**, 104109 (2009).
- <sup>2</sup>L. E. Cross, Flexoelectric effects: Charge separation in insulating solids subjected to elastic strain gradients, *J. Mater. Sci.* **41**, 53 (2006).
- <sup>3</sup>S. M. Kogan, Piezoelectric effect during inhomogeneous deformation and acoustic scattering of carriers in crystals, *Sov. Phys. Solid State* **5**, 2069 (1964).
- <sup>4</sup>E. V. Bursian and O. I. Zaikovsk, Changes in curvature of a ferroelectric film due to polarization, *Sov. Phys. Solid State. USSR* **10**, 1121 (1968).
- <sup>5</sup>A. K. Tagantsev, Piezoelectricity and flexoelectricity in crystalline dielectrics, *Phys. Rev. B* **34**, 5883 (1986).
- <sup>6</sup>W. Ma and L. E. Cross, Large flexoelectric polarization in ceramic lead magnesium niobate, *Appl. Phys. Lett.* **79**, 4420 (2001).

- <sup>7</sup>W. Ma and L. E. Cross, Flexoelectricity of barium titanate, *Appl. Phys. Lett.* **88**, 232902 (2006).
- <sup>8</sup>P. Zubko, G. Catalan and A. Buckley, Erratum: Strain-gradient-induced polarization in SrTiO<sub>3</sub> single crystals [*Phys. Rev. Lett.* **99**, 167601 (2007)], *Phys. Rev. Lett.* **100**, 199906 (2008).
- <sup>9</sup>G. Catalan, A. Lubk and A. H. G. Vlooswijk, Flexoelectric rotation of polarization in ferroelectric thin films, *Nat. Mater.* **10**, 963 (2011).
- <sup>10</sup>G. Catalan and B. Noheda, Temperature-dependent polarization in a non-polar crystal, *Nature* **575**, 600 (2019).
- <sup>11</sup>H. Lu, C. W. Bark and D. Esque De Los Ojos, Mechanical writing of ferroelectric polarization, *Science* **336**, 59 (2012).
- <sup>12</sup>M. M. Yang, D. J. Kim and M. Alexe, Flexo-photovoltaic effect, *Science* **360**, 904 (2018).
- <sup>13</sup>L. Shu, S. Ke and L. Fei, Photoflexoelectric effect in halide perovskites, *Nat. Mater.* **19**, 605 (2020).
- <sup>14</sup>V. Harbola, S. Crossley and S. S. Hong, Strain gradient elasticity in SrTiO<sub>3</sub> membranes: Bending versus stretching, *Nano Lett.* **21**, 2470 (2021).
- <sup>15</sup>R. Roy, D. Nečas and L. Zajíčková, Evidence of flexoelectricity in graphene nanobubbles created by tip induced electric field, *Carbon* **179**, 677 (2021).
- <sup>16</sup>J. Jiang, Z. Chen, Y. Hu, G.-C. Wang and J. Shi, Flexo-photovoltaic effect in MoS<sub>2</sub>, *Nat. Nanotechnol.* **16**, 894 (2021).
- <sup>17</sup>D. Lu, D. J. Baek and S. S. Hong, Synthesis of freestanding single-crystal perovskite films and heterostructures by etching of sacrificial water-soluble layers, *Nat. Mater.* **15**, 1255 (2016).
- <sup>18</sup>Y. Kim, K. Lee and B. O. Alawode, Remote epitaxy through graphene enables two-dimensional material-based layer transfer, *Nature* **544**, 340 (2017).
- <sup>19</sup>J. Hong and D. Vanderbilt, First-principles theory and calculation of flexoelectricity, *Phys. Rev. B* **88**, 174107 (2013).
- <sup>20</sup>Z. L. Wang, Y. Zhang and W. Hu, Flexoelectric effect. In *Piezotronics and Piezo-Phototronics, Microtechnology and MEMS*, Vol. 140, No. 529 (Springer, Cham, 2023).
- <sup>21</sup>W. Ma and L. E. Cross, Flexoelectric polarization of barium strontium titanate in the paraelectric state, *Appl. Phys. Lett.* **81**, 3440 (2002).
- <sup>22</sup>J. Narvaez, S. Saremi and J. Hong, Large flexoelectric anisotropy in paraelectric barium titanate, *Phys. Rev. Lett.* **115**, 037601 (2015).
- <sup>23</sup>D. Lee, A. Yoon and S. Y. Jang, Giant flexoelectric effect in ferroelectric epitaxial thin films, *Phys. Rev. Lett.* **107**, 057602 (2011).
- <sup>24</sup>Y. Wang, C. Guo and M. Chen, Mechanically driven reversible polarization switching in imprinted BiFeO<sub>3</sub> thin films, *Adv. Funct. Mater.* **33**, 2213787 (2023).
- <sup>25</sup>O. Diéguez, S. Tinte, A. Antons, C. Bungaro, J. B. Neaton, K. M. Rabe and D. Vanderbilt, *Ab initio* study of the phase diagram of epitaxial BaTiO<sub>3</sub>, *Phys. Rev. B* **69**, 212101 (2004).
- <sup>26</sup>J. H. Haeni, P. Irvin and W. Chang, Room-temperature ferroelectricity in strained SrTiO<sub>3</sub>, *Nature* **430**, 758 (2004).
- <sup>27</sup>C. Tan, J. Chen and X. J. Wu, Epitaxial growth of hybrid nanostructures, *Nat. Rev. Mater.* **3**, 1 (2018).
- <sup>28</sup>B. Lalmi, H. Oughaddou, H. Enriquez, B. Ealet and B. Aufray, Epitaxial growth of a silicene sheet, *Appl. Phys. Lett.* **97**, 223109 (2010).
- <sup>29</sup>A. K. Tagantsev, Electric polarization in crystals and its response to thermal and elastic perturbations, *Phase Transit.* **35**, 119 (1991).
- <sup>30</sup>A. Gruverman, B. J. Rodriguez and A. I. Kingon, Mechanical stress effect on imprint behavior of integrated ferroelectric capacitors, *Appl. Phys. Lett.* **83**, 728 (2003).
- <sup>31</sup>M. E. Lines and A. M. Glass, *Principles and Applications of Ferroelectrics and Related Materials* (Oxford University Press, 2001).
- <sup>32</sup>B. Wang, Y. Gu and S. Zhang, Flexoelectricity in solids: Progress, challenges, and perspectives, *Prog. Mater. Sci.* **106**, 100570 (2019).
- <sup>33</sup>Y. Tang, Y. L. Zhu, X. Ma and Z. Hong, A coherently strained monoclinic [111] PbTiO<sub>3</sub> film exhibiting zero Poisson's ratio state, *Adv. Funct. Mater.* **29**, 1901687 (2019).
- <sup>34</sup>J. Xu, W. Zheng and Y. Yu, Effects of flexoelectric polarization on surface potential of dielectric thin-film heterostructures: A comparative study, *Appl. Phys. Lett.* **121**, 203502 (2022).
- <sup>35</sup>E. J. Guo, R. Roth and S. Das, Strain induced low mechanical switching force in ultrathin PbZr<sub>0.2</sub>Ti<sub>0.8</sub>O<sub>3</sub> films, *Appl. Phys. Lett.* **105**, 012903 (2014).
- <sup>36</sup>Z. Wen, X. Qiu and C. Li, Mechanical switching of ferroelectric polarization in ultrathin BaTiO<sub>3</sub> films: The effects of epitaxial strain, *Appl. Phys. Lett.* **104**, 042907 (2014).
- <sup>37</sup>D. Lee, H. Lu and Y. Gu, Emergence of room-temperature ferroelectricity at reduced dimensions, *Science* **349**, 1314 (2015).
- <sup>38</sup>A. Gómez, J. M. Vila-Fungueiriño and R. Moalla, Electric and mechanical switching of ferroelectric and resistive states in semi-conducting BaTiO<sub>3-δ</sub> films on silicon, *Small* **13**, 1701614 (2017).
- <sup>39</sup>H. Lu, S. Liu and Z. Ye, Asymmetry in mechanical polarization switching, *Appl. Phys. Lett.* **110**, 222903 (2017).
- <sup>40</sup>H. Lu, D. Lee and K. Klyukin, Tunneling hot spots in ferroelectric SrTiO<sub>3</sub>, *Nano Lett.* **18**, 491 (2018).
- <sup>41</sup>S. M. Park, B. Wang and S. Das, Selective control of multiple ferroelectric switching pathways using a trailing flexoelectric field, *Nat. Nanotechnol.* **13**, 366 (2018).
- <sup>42</sup>S. Das, B. Wang and T. R. Paudel, Enhanced flexoelectricity at reduced dimensions revealed by mechanically tunable quantum tunnelling, *Nat. Commun.* **10**, 537 (2019).
- <sup>43</sup>Z. Guan, Y. K. Li and Y. F. Zhao, Mechanical polarization switching in Hf<sub>0.5</sub>Zr<sub>0.5</sub>O<sub>2</sub> thin film, *Nano Lett.* **22**, 4792 (2022).
- <sup>44</sup>Y. Xia, Y. Ji and Y. Liu, Controllable piezo-flexoelectric effect in ferroelectric Ba<sub>0.7</sub>Sr<sub>0.3</sub>TiO<sub>3</sub> materials for harvesting vibration energy, *ACS Appl. Mater. Interfaces* **14**, 32 (2022).
- <sup>45</sup>A. Tripathy, B. Saravanakumar and S. Mohanty, Comprehensive review on flexoelectric energy harvesting technology: Mechanisms, device configurations, and potential applications, *ACS Appl. Electron. Mater.* **3**, 2898 (2021).
- <sup>46</sup>H. Han, Y. Ji and L. Wu, Coupling enhancement of a flexible BiFeO<sub>3</sub> film-based nanogenerator for simultaneously scavenging light and vibration energies, *Nano-Micro Lett.* **14**, 198 (2022).
- <sup>47</sup>S. Huang, L. Qi and W. Huang, Flexoelectricity in dielectrics: Materials, structures and characterizations, *J. Adv. Dielect.* **8**, 1830002 (2018).
- <sup>48</sup>U. K. Bhaskar, N. Banerjee and A. Abdollahi, A flexoelectric microelectromechanical system on silicon, *Nat. Nanotechnol.* **11**, 263 (2016).

- <sup>49</sup>M. Wu, Z. Jiang and X. Lou, Flexoelectric thin-film photo-detectors, *Nano Lett.* **21**, 2946 (2021).
- <sup>50</sup>W. Huang, S. Yang and N. Zhang, Cracks monitoring and characterization by Ba<sub>0.64</sub>Sr<sub>0.36</sub>TiO<sub>3</sub> flexoelectric strain gradient sensors, *Proc. SPIE* **9061**, 310 (2014).
- <sup>51</sup>X. Jiang, W. Huang and S. Zhang, Flexoelectric nano-generator: Materials, structures and devices, *Nano Energy* **2**, 1079 (2013).
- <sup>52</sup>P. Lukashev and R. F. Sabirianov, Flexomagnetic effect in frustrated triangular magnetic structures, *Phys. Rev. B* **82**, 094417 (2010).
- <sup>53</sup>S. Sidhardh and M. C. Ray, Flexomagnetic response of nanostructures, *J. Appl. Phys.* **124**, 244101 (2018).
- <sup>54</sup>T. Choi, S. Lee and Y. J. Choi, Switchable ferroelectric diode and photovoltaic effect in BiFeO<sub>3</sub>, *Science* **324**, 63 (2009).
- <sup>55</sup>S. Y. Yang, J. Seidel and S. J. Byrnes, Above-bandgap voltages from ferroelectric photovoltaic devices, *Nat. Nanotechnol.* **5**, 143 (2010).
- <sup>56</sup>M. Alexe and D. Hesse, Tip-enhanced photovoltaic effects in bismuth ferrite, *Nat. Commun.* **2**, 256 (2011).
- <sup>57</sup>L. You, F. Zheng and L. Fang, Enhancing ferroelectric photovoltaic effect by polar order engineering, *Sci. Adv.* **4**, eaat3438 (2018).
- <sup>58</sup>M. M. Seyfour and D. Wang, Recent progress in bismuth ferrite-based thin films as a promising photovoltaic material, *Crit. Rev. Solid State Mater. Sci.* **46**, 83 (2021).
- <sup>59</sup>Z. Sun, J. Wei and Y. Li, Coupling oxygen vacancy gradient distribution and flexoelectric effects for enhanced photovoltaic performance in bismuth ferrite films, *Inorg. Chem. Front.* **10**, 1315 (2023).
- <sup>60</sup>J. Wang, R. Zhu and J. Ma, Photoenhanced electroresistance at dislocation-mediated phase boundary, *ACS Appl. Mater. Interfaces* **14**, 18662 (2022).
- <sup>61</sup>Y. Li, C. Adamo and P. Chen, Giant optical enhancement of strain gradient in ferroelectric BiFeO<sub>3</sub> thin films and its physical origin, *Sci. Rep.* **5**, 16650 (2015).
- <sup>62</sup>F. Zhang, P. Lv and Y. Zhang, Modulating the electrical transport in the two-dimensional electron gas at LaAlO<sub>3</sub>/SrTiO<sub>3</sub> heterostructures by interfacial flexoelectricity, *Phys. Rev. Lett.* **122**, 257601 (2019).
- <sup>63</sup>L. Shu, R. Liang and Z. Rao, Flexoelectric materials and their related applications: A focused review, *J. Adv. Ceram.* **8**, 153 (2019).
- <sup>64</sup>W. Ma, Flexoelectricity: Strain gradient effects in ferroelectrics, *Phys. Scr.* **180**, 2007 (2007).
- <sup>65</sup>G. Catalan, B. Noheda and J. McAneney, Strain gradients in epitaxial ferroelectrics, *Phys. Rev. B* **72**, 020102 (2005).
- <sup>66</sup>P. W. Shao, H. J. Liu and Y. Sun, Flexoelectric domain walls originated from structural phase transition in epitaxial BiVO<sub>4</sub> films, *Small* **18**, 2107540 (2022).
- <sup>67</sup>Y. P. Feng, R. J. Jiang and Y. L. Zhu, Strain coupling of ferroelastic domains and misfit dislocations in [101]-oriented ferroelectric PbTiO<sub>3</sub> films, *RSC Adv.* **12**, 20423 (2022).
- <sup>68</sup>G. F. Nataf, M. Guennou and J. M. Gregg, Domain-wall engineering and topological defects in ferroelectric and ferroelastic materials, *Nat. Rev. Phys.* **2**, 634 (2020).
- <sup>69</sup>R. K. Vasudevan, Y. Cao and N. Laanait, Field enhancement of electronic conductance at ferroelectric domain walls, *Nat. Commun.* **8**, 1318 (2017).
- <sup>70</sup>X. Ren, Large electric-field-induced strain in ferroelectric crystals by point-defect-mediated reversible domain switching, *Nat. Mater.* **3**, 91 (2004).
- <sup>71</sup>A. Ohtomo and H. Y. Hwang, A high-mobility electron gas at the LaAlO<sub>3</sub>/SrTiO<sub>3</sub> heterointerface, *Nature* **427**, 423 (2004).
- <sup>72</sup>P. Yu, W. Luo and D. Yi, Interface control of bulk ferroelectric polarization, *Proc. Natl. Acad. Sci.* **109**, 9710 (2012).
- <sup>73</sup>M. W. Chu, I. Szafraniak and R. Scholz, Impact of misfit dislocations on the polarization instability of epitaxial nanostructured ferroelectric perovskites, *Nat. Mater.* **3**, 87 (2004).
- <sup>74</sup>V. Nagarajan, C. L. Jia and H. Kohlstedt, Misfit dislocations in nanoscale ferroelectric heterostructures, *Appl. Phys. Lett.* **86**, 192910 (2005).
- <sup>75</sup>L. W. Martin and A. M. Rappe, Thin-film ferroelectric materials and their applications, *Nat. Rev. Mater.* **2**, 1 (2016).
- <sup>76</sup>B. C. Jeon, D. Lee and M. H. Lee, Flexoelectric effect in the reversal of self-polarization and associated changes in the electronic functional properties of BiFeO<sub>3</sub> thin films, *Adv. Mater.* **25**, 5643 (2013).
- <sup>77</sup>W. Geng, Y. Wang and Y. Tang, Atomic-scale tunable flexoelectric couplings in oxide multiferroics, *Nano Lett.* **21**, 9601 (2021).
- <sup>78</sup>T. D. Nguyen, S. Mao and Y. W. Yeh, Nanoscale flexoelectricity, *Adv. Mater.* **25**, 946 (2013).
- <sup>79</sup>L. Shu, Z. Wang and R. Liang, Intrinsic flexoelectricity of van der Waals epitaxial thin films, *Phys. Rev. B* **106**, 024108 (2022).
- <sup>80</sup>L. Dai, J. Zhao and J. Li, Highly heterogeneous epitaxy of flexoelectric BaTiO<sub>3- $\delta$</sub>  membrane on Ge, *Nat. Commun.* **13**, 2990 (2022).
- <sup>81</sup>Y. Tang, Y. Zhu and B. Wu, Periodic polarization waves in a strained, highly polar ultrathin SrTiO<sub>3</sub>, *Nano Lett.* **21**, 6274 (2021).
- <sup>82</sup>K. E. Kim, S. Jeong and K. Chu, Configurable topological textures in strain graded ferroelectric nanoplates, *Nat. Commun.* **9**, 403 (2018).
- <sup>83</sup>W. Geng, X. Guo and Y. Zhu, Rhombohedral-orthorhombic ferroelectric morphotropic phase boundary associated with a polar vortex in BiFeO<sub>3</sub> films, *ACS Nano* **12**, 11098 (2018).
- <sup>84</sup>Y. L. Tang, Y. L. Zhu and X. L. Ma, Observation of a periodic array of flux-closure quadrants in strained ferroelectric PbTiO<sub>3</sub> films, *Science* **348**, 547 (2015).
- <sup>85</sup>S. Das, Y. L. Tang and Z. Hong, Observation of room-temperature polar skyrmions, *Nature* **568**, 368 (2019).
- <sup>86</sup>Y. J. Wang, Y. P. Feng and Y. L. Zhu, Polar meron lattice in strained oxide ferroelectrics, *Nat. Mater.* **19**, 881 (2020).
- <sup>87</sup>K. Chu, B. K. Jang and J. H. Sung, Enhancement of the anisotropic photocurrent in ferroelectric oxides by strain gradients, *Nat. Nanotechnol.* **10**, 972 (2015).
- <sup>88</sup>Y. Zhang, J. Li and D. Fang, Size dependent domain configuration and electric field driven evolution in ultrathin ferroelectric films: A phase field investigation, *J. Appl. Phys.* **107**, 034107 (2010).
- <sup>89</sup>M. M. Yang, A. N. Iqbal and J. J. P. Peters, Strain-gradient mediated local conduction in strained bismuth ferrite films, *Nat. Commun.* **10**, 2791 (2019).
- <sup>90</sup>Y. D. Liou, Y. Y. Chiu and R. T. Hart, Deterministic optical control of room temperature multiferroicity in BiFeO<sub>3</sub> thin films, *Nat. Mater.* **18**, 580 (2019).



- <sup>91</sup>J. Junquera and P. Ghosez, Critical thickness for ferroelectricity in perovskite ultrathin films, *Nature* **422**, 506 (2003).
- <sup>92</sup>Y. L. Tang, Y. L. Zhu and M. J. Zou, Coexisting morphotropic phase boundary and giant strain gradient in BiFeO<sub>3</sub> films, *J. Appl. Phys.* **129**, 184101 (2021).
- <sup>93</sup>P. Gao, S. Yang and R. Ishikawa, Atomic-scale measurement of flexoelectric polarization at SrTiO<sub>3</sub> dislocations, *Phys. Rev. Lett.* **120**, 267601 (2018).
- <sup>94</sup>J. Zhang, C. Wang and C. Bowen, Piezoelectric effects and electromechanical theories at the nanoscale, *Nanoscale* **6**, 13314 (2014).
- <sup>95</sup>A. K. Tagantsev, G. Gerra and N. Setter, Short-range and long-range contributions to the size effect in metal-ferroelectric-metal heterostructures, *Phys. Rev. B* **77**, 174111 (2008).
- <sup>96</sup>W. Chen, Y. Zheng and X. Feng, Utilizing mechanical loads and flexoelectricity to induce and control complicated evolution of domain patterns in ferroelectric nanofilms, *J. Mech. Phys. Solids* **79**, 108 (2015).
- <sup>97</sup>S. Dai, M. Gharbi and P. Sharma, Surface piezoelectricity: Size effects in nanostructures and the emergence of piezoelectricity in non-piezoelectric materials, *J. Appl. Phys.* **110**, 104305 (2011).
- <sup>98</sup>S. Shen and S. Hu, A theory of flexoelectricity with surface effect for elastic dielectrics, *J. Mech. Phys. Solids* **58**, 665 (2010).
- <sup>99</sup>I. S. Vorotiahin, E. A. Eliseev and Q. Li, Tuning the polar states of ferroelectric films via surface charges and flexoelectricity, *Acta Mater.* **137**, 85 (2017).
- <sup>100</sup>C. Qi and X. Wang, Surface effects on domain switching of a ferroelectric thin film under local mechanical load: A phase-field investigation, *J. Appl. Phys.* **129**, 094101 (2021).
- <sup>101</sup>W. Hou, S. A. Chowdhury and A. Dey, Nonvolatile ferroelastic strain from flexoelectric internal bias engineering, *Phys. Rev. Appl.* **17**, 024013 (2022).
- <sup>102</sup>Z. Zheng, P. Huang and F. Wang, Shape memory effect based thermal cycling induced flexoelectricity for energy harvesting, *Scr. Mater.* **194**, 113701 (2021).
- <sup>103</sup>P. Sharma, S. Ryu and Z. Viskadourakis, Electromechanics of ferroelectric-like behavior of LaAlO<sub>3</sub> thin films, *Adv. Funct. Mater.* **25**, 6538 (2015).
- <sup>104</sup>P. Sharma, S. Ryu and J. D. Burton, Mechanical tuning of LaAlO<sub>3</sub>/SrTiO<sub>3</sub> interface conductivity, *Nano Lett.* **15**, 3547 (2015).
- <sup>105</sup>S. Das, B. Wang and Y. Cao, Controlled manipulation of oxygen vacancies using nanoscale flexoelectricity, *Nat. Commun.* **8**, 615 (2017).
- <sup>106</sup>S. M. Park, B. Wang and T. Paudel, Colossal flexoresistance in dielectrics, *Nat. Commun.* **11**, 2586 (2020).
- <sup>107</sup>H. Lu, D. J. Kim and C. W. Bark, Mechanically-induced resistive switching in ferroelectric tunnel junctions, *Nano Lett.* **12**, 6289 (2012).
- <sup>108</sup>A. V. Ievlev, A. N. Morozovska and E. A. Eliseev, Ionic field effect and memristive phenomena in single-point ferroelectric domain switching, *Nat. Commun.* **5**, 4545 (2014).
- <sup>109</sup>Y. Kim, S. Bühlmann and S. Hong, Injection charge assisted polarization reversal in ferroelectric thin films, *Appl. Phys. Lett.* **90**, 072910 (2007).
- <sup>110</sup>A. V. Ievlev, A. N. Morozovska and V. Y. Shur, Ferroelectric switching by the grounded scanning probe microscopy tip, *Phys. Rev. B* **91**, 214109 (2015).
- <sup>111</sup>J. Liu, W. Chen and M. Wu, Bidirectional mechanical switching window in ferroelectric thin films predicted by first-principle-based simulations, *npj Comput. Mater.* **8**, 137 (2022).
- <sup>112</sup>W. Ming, B. Huang and S. Zheng, Flexoelectric engineering of van der Waals ferroelectric CuInP<sub>2</sub>S<sub>6</sub>, *Sci. Adv.* **8**, eabq1232 (2022).
- <sup>113</sup>A. Abdollahi, N. Domingo and I. Arias, Converse flexoelectricity yields large piezoresponse force microscopy signals in non-piezoelectric materials, *Nat. Commun.* **10**, 1266 (2019).
- <sup>114</sup>A. N. Morozovska, E. A. Eliseev and N. Balke, Local probing of ionic diffusion by electrochemical strain microscopy: Spatial resolution and signal formation mechanisms, *J. Appl. Phys.* **108**, 053712 (2010).
- <sup>115</sup>A. N. Morozovska, E. A. Eliseev and G. S. Svechnikov, Nano-scale electromechanics of paraelectric materials with mobile charges: Size effects and nonlinearity of electromechanical response of SrTiO<sub>3</sub> films, *Phys. Rev. B* **84**, 045402 (2011).
- <sup>116</sup>N. Balke, S. Jesse and Y. Kim, Decoupling electrochemical reaction and diffusion processes in ionically-conductive solids on the nanometer scale, *ACS Nano* **4**, 7349 (2010).
- <sup>117</sup>S. Jesse, A. Kumar and T. M. Arruda, Electrochemical strain microscopy: Probing ionic and electrochemical phenomena in solids at the nanometer level, *MRS Bull.* **37**, 651 (2012).
- <sup>118</sup>Y. S. Oh, X. Luo and F. T. Huang, Experimental demonstration of hybrid improper ferroelectricity and the presence of abundant charged walls in (Ca, Sr)<sub>3</sub>Ti<sub>2</sub>O<sub>7</sub> crystals, *Nat. Mater.* **14**, 407 (2015).
- <sup>119</sup>Y. Cao, J. Shen and C. Randall, Effect of multi-domain structure on ionic transport, electrostatics, and current evolution in BaTiO<sub>3</sub> ferroelectric capacitor, *Acta Mater.* **112**, 224 (2016).
- <sup>120</sup>M. Y. Zhuravlev, R. F. Sabirianov and S. S. Jaswal, Giant electroresistance in ferroelectric tunnel junctions, *Phys. Rev. Lett.* **94**, 246802 (2005).
- <sup>121</sup>J. P. Velev, J. D. Burton and M. Y. Zhuravlev, Predictive modelling of ferroelectric tunnel junctions, *npj Comput. Mater.* **2**, 1 (2016).
- <sup>122</sup>A. Gruverman, D. Wu and H. Lu, Tunneling electroresistance effect in ferroelectric tunnel junctions at the nanoscale, *Nano Lett.* **9**, 3539 (2009).
- <sup>123</sup>A. K. Geim and I. V. Grigorieva, Van der Waals heterostructures, *Nature* **499**, 419 (2013).
- <sup>124</sup>J. H. Ahn, H. S. Kim and K. J. Lee, Heterogeneous three-dimensional electronics by use of printed semiconductor nanomaterials, *Science* **314**, 1754 (2006).
- <sup>125</sup>K. H. Yim, Z. Zheng and Z. Liang, Efficient conjugated-polymer optoelectronic devices fabricated by thin-film transfer-printing technique, *Adv. Funct. Mater.* **18**, 1012 (2008).
- <sup>126</sup>H. Kum, D. Lee and W. Kong, Epitaxial growth and layer-transfer techniques for heterogeneous integration of materials for electronic and photonic devices, *Nat. Electron.* **2**, 439 (2019).
- <sup>127</sup>Y. Lun, S. Xu and X. Wang, Flexoelectricity in self-rolling freestanding heterogeneous films, *Int. J. Solids Struct.* **271**, 112223 (2023).
- <sup>128</sup>G. Dong, S. Li and M. Yao, Super-elastic ferroelectric single-crystal membrane with continuous electric dipole rotation, *Science* **366**, 475 (2019).
- <sup>129</sup>S. Cai, Y. Lun and D. Ji, Enhanced polarization and abnormal flexural deformation in bent freestanding perovskite oxides, *Nat. Commun.* **13**, 5116 (2022).
- <sup>130</sup>Q. Huang, Z. Fan and J. Rao, Significant modulation of ferroelectric photovoltaic behavior by a giant macroscopic flexoelectric effect induced by strain-relaxed epitaxy, *Adv. Electron. Mater.* **8**, 2100612 (2022).

- <sup>131</sup>D. Ji, S. Cai and T. R. Paudel, Freestanding crystalline oxide perovskites down to the monolayer limit, *Nature* **570**, 87 (2019).
- <sup>132</sup>R. Guo, L. You and W. Lin, Continuously controllable photoconductance in freestanding BiFeO<sub>3</sub> by the macroscopic flexoelectric effect, *Nat. Commun.* **11**, 2571 (2020).
- <sup>133</sup>M. Zhang, D. Yan and J. Wang, Ultrahigh flexoelectric effect of 3D interconnected porous polymers: Modelling and verification, *J. Mech. Phys. Solids* **151**, 104396 (2021).
- <sup>134</sup>V. M. Ruiz, D. Olmos and J. González-Benito, PVDF/MWCNT nanocomposites with complex configurations prepared by solution blow spinning and their flexoelectric responses, *Polymer* **267**, 125669 (2023).
- <sup>135</sup>S. H. Bae, H. Kum and W. Kong, Integration of bulk materials with two-dimensional materials for physical coupling and applications, *Nat. Mater.* **18**, 550 (2019).
- <sup>136</sup>D. Geng and H. Y. Yang, Recent advances in growth of novel 2D materials: Beyond graphene and transition metal dichalcogenides, *Adv. Mater.* **30**, 1800865 (2018).
- <sup>137</sup>B. R. Tak, V. Gupta and A. K. Kapoor, Wearable gallium oxide solar-blind photodetectors on muscovite mica having ultrahigh photoresponsivity and detectivity with added high-temperature functionalities, *ACS Appl. Electron. Mater.* **1**, 2463 (2019).
- <sup>138</sup>M. Yen, Y. H. Lai and C. Y. Kuo, Mechanical modulation of colossal magnetoresistance in flexible epitaxial perovskite manganite, *Adv. Funct. Mater.* **30**, 2004597 (2020).
- <sup>139</sup>T. D. Ha, J. W. Chen and M. Yen, Dynamical strain-driven phase separation in flexible CoFe<sub>2</sub>O<sub>4</sub>/CoO exchange coupling system, *ACS Appl. Mater. Inter.* **12**, 46874 (2020).
- <sup>140</sup>M. Qi, Z. Yang and S. Chen, Asymmetric ground states in La<sub>0.67</sub>Sr<sub>0.33</sub>MnO<sub>3</sub>/BaTiO<sub>3</sub> heterostructures induced by flexoelectric bending, *Appl. Phys. Lett.* **120**, 233103 (2022).
- <sup>141</sup>W. Yang, S. Chen and X. Ding, Reducing threshold of ferroelectric domain switching in ultrathin two-dimensional CuInP<sub>2</sub>S<sub>6</sub> ferroelectrics via electrical–mechanical coupling, *J. Phys. Chem. Lett.* **14**, 379 (2023).
- <sup>142</sup>M. Osada and T. Sasaki, Exfoliated oxide nanosheets: New solution to nanoelectronics, *J. Mater. Chem. A* **19**, 2503 (2009).
- <sup>143</sup>R. Ma and T. Sasaki, Nanosheets of oxides and hydroxides: Ultimate 2D charge-bearing functional crystallites, *Adv. Mater.* **22**, 5082 (2010).
- <sup>144</sup>M. Osada and T. Sasaki, 2D Inorganic nanosheets: Two-dimensional dielectric nanosheets: Novel nanoelectronics from nanocrystal building blocks, *Adv. Mater.* **24**, 209 (2012).
- <sup>145</sup>L. P. Gor'kov and E. I. Rashba, Superconducting 2D system with lifted spin degeneracy: Mixed singlet-triplet state, *Phys. Rev. Lett.* **87**, 037004 (2001).
- <sup>146</sup>D. Awschalom and N. Samarth, Spintronics without magnetism, *Physics* **2**, 50 (2009).
- <sup>147</sup>B. J. Kim, H. Jin and S. J. Moon, Novel J eff = 1/2 Mott state induced by relativistic spin-orbit coupling in Sr<sub>2</sub>IrO<sub>4</sub>, *Phys. Rev. Lett.* **101**, 076402 (2008).
- <sup>148</sup>A. Shitade, H. Katsura and J. Kuneš, Quantum spin Hall effect in a transition metal oxide Na<sub>2</sub>IrO<sub>3</sub>, *Phys. Rev. Lett.* **102**, 256403 (2009).
- <sup>149</sup>P. Koirala, C. A. Mizzi and L. D. Marks, Direct observation of large flexoelectric bending at the nanoscale in lanthanide scandates, *Nano Lett.* **18**, 3850 (2018).
- <sup>150</sup>T. Leydecker, M. Herder and E. Pavlica, Flexible non-volatile optical memory thin-film transistor device with over 256 distinct levels based on an organic bicomponent blend, *Nat. Nanotechnol.* **11**, 769 (2016).
- <sup>151</sup>F. R. Fan, W. Tang and Z. L. Wang, Flexible nanogenerators for energy harvesting and self-powered electronics, *Adv. Mater.* **28**, 4283 (2016).
- <sup>152</sup>Z. L. Wang and J. Song, Piezoelectric nanogenerators based on zinc oxide nanowire arrays, *Science* **312**, 242 (2006).
- <sup>153</sup>X. Cao, Y. Xiong and J. Sun, Piezoelectric nanogenerators derived self-powered sensors for multifunctional applications and artificial intelligence, *Adv. Funct. Mater.* **31**, 2102983 (2021).
- <sup>154</sup>J. Briscoe and S. Dunn, Piezoelectric nanogenerators — a review of nanostructured piezoelectric energy harvesters, *Nano Energy* **14**, 15 (2015).
- <sup>155</sup>D. Hu, M. Yao and Y. Fan, Strategies to achieve high performance piezoelectric nanogenerators, *Nano Energy* **55**, 288 (2019).
- <sup>156</sup>S. Rajeevan, S. John and S. C. George, Polyvinylidene fluoride: A multifunctional polymer in supercapacitor applications, *J. Power Sources* **504**, 230037 (2021).
- <sup>157</sup>Y. Li, Q. Zhou and J. Wu, Controllably grown single-crystal films as flexoelectric nanogenerators for continuous direct current output, *npj Flex. Electron.* **6**, 88 (2022).
- <sup>158</sup>L. Molina-Luna, S. Wang and Y. Pivak, Enabling nanoscale flexoelectricity at extreme temperature by tuning cation diffusion, *Nat. Commun.* **9**, 1 (2018).
- <sup>159</sup>E. A. Eliseev, A. N. Morozovska and V. V. Khist, Effective flexoelectric and flexomagnetic response of ferroics, *Phys. Solid State* **70**, 237 (2019).
- <sup>160</sup>P. Zubko, G. Catalan and A. Buckley, Strain-gradient-induced polarization in SrTiO<sub>3</sub> single crystals, *Phys. Rev. Lett.* **99**, 167601 (2007).
- <sup>161</sup>Y. Geng, N. Lee and Y. J. Choi, Collective magnetism at multiferroic vortex domain walls, *Nano Lett.* **12**, 6055 (2012).
- <sup>162</sup>M. Hehn, K. Ounadjela and J. P. Bucher, Nanoscale magnetic domains in mesoscopic magnets, *Science* **272**, 1782 (1996).
- <sup>163</sup>T. Jia, H. Kimura and Z. Cheng, Mechanical force involved multiple fields switching of both local ferroelectric and magnetic domain in a Bi<sub>5</sub>Ti<sub>3</sub>FeO<sub>15</sub> thin film, *NPG Asia Mater.* **9**, e349 (2017).
- <sup>164</sup>I. I. Naumov and A. M. Bratkovsky, Gap opening in graphene by simple periodic inhomogeneous strain, *Phys. Rev. B* **84**, 245444 (2011).
- <sup>165</sup>Y. Ling, X. Yu and S. Yuan, Flexomagnetic effect enhanced ferromagnetism and magnetoelectrochemistry in freestanding high-entropy alloy films, *ACS Nano* **3c05255** (2023).
- <sup>166</sup>S. R. Spurgeon, J. D. Sloppy and D. M. Kepaptsoglou, Thickness-dependent crossover from charge- to strain-mediated magnetoelectric coupling in ferromagnetic/piezoelectric oxide heterostructures, *ACS Nano* **8**, 894 (2014).
- <sup>167</sup>A. Ghobadi, Y. T. Beni and H. Golestanian, Size dependent thermo-electro-mechanical nonlinear bending analysis of flexoelectric nano-plate in the presence of magnetic field, *Int. J. Mech. Sci.* **152**, 118 (2019).
- <sup>168</sup>A. P. Pyatakov and A. K. Zvezdin, Flexomagnetolectric interaction in multiferroics, *Eur. Phys. J. B* **71**, 419 (2009).
- <sup>169</sup>V. Goian, S. Kamba and J. Hlinka, Polar phonon mixing in magnetoelectric EuTiO<sub>3</sub>, *Eur. Phys. J. B* **71**, 429 (2009).
- <sup>170</sup>S. W. Cheong and M. Mostovoy, Multiferroics: A magnetic twist for ferroelectricity, *Nat. Mater.* **6**, 13 (2007).

- <sup>171</sup>E. A. Eliseev, A. N. Morozovska and M. D. Glinchuk, Spontaneous flexoelectric/flexomagnetic effect in nanoferroics, *Phys. Rev. B* **79**, 165433 (2009).
- <sup>172</sup>R. Basutkar, S. Sidhardh and M. C. Ray, Static analysis of flexoelectric nanobeams incorporating surface effects using element free Galerkin method, *Eur. J. Mech. A Solids* **76**, 13 (2019).
- <sup>173</sup>N. Zhang, S. Zheng and D. Chen, Size-dependent static bending of flexomagnetic nanobeams, *J. Appl. Phys.* **126** (2019).
- <sup>174</sup>M. Malikan, T. Wiczenbach and V. A. Eremeyev, On thermal stability of piezo-flexomagnetic microbeams considering different temperature distributions, *Continuum Mech. Therm.* **33**, 1281 (2021).
- <sup>175</sup>M. Malikan, T. Wiczenbach and V. A. Eremeyev, Thermal buckling of functionally graded piezomagnetic micro- and nanobeams presenting the flexomagnetic effect, *Continuum Mech. Therm.* **34**, 1051 (2022).
- <sup>176</sup>H. Momeni-Khabisi and M. Tahani, A size-dependent study on buckling and post-buckling behavior of imperfect piezo-flexomagnetic nano-plate strips, *Adv. Nano Res.* **12**, 427 (2022).
- <sup>177</sup>H. Momeni-Khabisi and M. Tahani, Coupled thermal stability analysis of piezomagnetic nano-sensors and nano-actuators considering the flexomagnetic effect, *Eur. J. Mech. A Solids* **97**, 104773 (2023).
- <sup>178</sup>D. Cao, C. Wang and F. Zheng, High-efficiency ferroelectric-film solar cells with an n-type Cu<sub>2</sub>O cathode buffer layer, *Nano Lett.* **12**, 2803 (2012).
- <sup>179</sup>W. Huang, C. Harnagea and D. Benetti, Multiferroic Bi<sub>2</sub>FeCrO<sub>6</sub> based p-i-n heterojunction photovoltaic devices, *J. Mater. Chem. A* **5**, 10355 (2017).
- <sup>180</sup>X. Yang, X. Su and M. Shen, Enhancement of photocurrent in ferroelectric films via the incorporation of narrow bandgap nanoparticles, *Adv. Mater.* **24**, 1202 (2012).
- <sup>181</sup>N. Ma, K. Zhang and Y. Yang, Photovoltaic-pyroelectric coupled effect induced electricity for self-powered photodetector system, *Adv. Mater.* **29**, 1703694 (2017).
- <sup>182</sup>J. Qi, N. Ma and Y. Yang, Photovoltaic-pyroelectric coupled effect based nanogenerators for self-powered photodetector system, *Adv. Mater. Interfaces* **5**, 1701189 (2018).
- <sup>183</sup>L. Wang, S. Liu and X. Feng, Flexoelectronics of centrosymmetric semiconductors, *Nat. Nanotechnol.* **15**, 661 (2020).
- <sup>184</sup>F. Sun, D. Chen and X. Gao, Emergent strain engineering of multiferroic BiFeO<sub>3</sub> thin films, *J. Materiomics* **7**, 281 (2021).
- <sup>185</sup>C. Yang, J. Qian and Y. Han, Design of an all-inorganic flexible Na<sub>0.5</sub>Bi<sub>0.5</sub>TiO<sub>3</sub>-based film capacitor with giant and stable energy storage performance, *J. Mater. Chem. A* **7**, 22366 (2019).
- <sup>186</sup>G. Zhong and J. Li, Muscovite mica as a universal platform for flexible electronics, *J. Materiomics* **6**, 455 (2020).
- <sup>187</sup>C. Yang, Y. Han and J. Qian, Flexible, temperature-resistant, and fatigue-free ferroelectric memory based on Bi (Fe<sub>0.93</sub>Mn<sub>0.05</sub>Ti<sub>0.02</sub>)O<sub>3</sub> thin film, *ACS Appl. Mater. Interfaces* **11**, 12647 (2019).
- <sup>188</sup>J. Tian, Y. Zhang and Z. Fan, Nanoscale phase mixture and multifield-induced topotactic phase transformation in SrFeO<sub>x</sub>, *ACS Appl. Mater. Interfaces* **12**, 21883 (2020).
- <sup>189</sup>K. Liu, T. Wu and L. Xu, Flexo-photocatalysis in centrosymmetric semiconductors, *Nano Res.* **1**, 9 (2023).
- <sup>190</sup>H. Zou, C. Zhang and H. Xue, Boosting the solar cell efficiency by flexo-photovoltaic effect? *ACS Nano* **13**, 12259 (2019).
- <sup>191</sup>D. Pu, M. A. Anwar and J. Zhou, Enhanced photovoltaic effect in graphene-silicon Schottky junction under mechanical manipulation, *Appl. Phys. Lett.* **122**, 041102 (2023).
- <sup>192</sup>L. Sun, L. Zhu and C. Zhang, Mechanical manipulation of silicon-based Schottky diodes via flexoelectricity, *Nano Energy* **83**, 105855 (2021).
- <sup>193</sup>C. Wang, Y. Zhang and B. Zhang, Flexophotovoltaic effect in potassium sodium niobate/poly (vinylidene fluoride-trifluoroethylene) nanocomposite, *Adv. Sci.* **8**, 2004554 (2021).
- <sup>194</sup>Z. Jiang, Z. Xu and Z. Xi, Flexoelectric-induced photovoltaic effects and tunable photocurrents in flexible LaFeO<sub>3</sub> epitaxial heterostructures, *J. Materiomics* **8**, 281 (2022).
- <sup>195</sup>Y. J. Zhang, T. Ideue and M. Onga, Enhanced intrinsic photovoltaic effect in tungsten disulfide nanotubes, *Nature* **570**, 349 (2019).
- <sup>196</sup>J. Narvaez, F. Vasquez-Sancho and G. Catalan, Enhanced flexoelectric-like response in oxide semiconductors, *Nature* **538**, 219 (2016).
- <sup>197</sup>X. Chen et al., Bulk photovoltaic effect in two-dimensional ferroelectric semiconductor *a*-In<sub>2</sub>Se<sub>3</sub>, preprint (2023), arXiv:2308.08382.
- <sup>198</sup>Q. Ma, X. Wen and L. Lv, On the flexoelectric-like effect of Nb-doped SrTiO<sub>3</sub> single crystals, *Appl. Phys. Lett.* **123**, 082902 (2023).
- <sup>199</sup>Y. Xia, H. Dan and Y. Ji, Flexible BaTiO<sub>3</sub> thin film-based coupled nanogenerator for simultaneously scavenging light and vibration energies, *ACS Appl. Mater. Interfaces* **15**, 23226 (2023).
- <sup>200</sup>D. Guo, P. Guo and L. Ren, Silicon flexoelectronic transistors, *Sci. Adv.* **9**, eadd3310 (2023).
- <sup>201</sup>L. Yu, A. Ruzsinszky and J. P. Perdew, Bending two-dimensional materials to control charge localization and Fermi-level shift, *Nano Lett.* **16**, 2444 (2016).
- <sup>202</sup>Y. H. Shen, Y. X. Song and W. Y. Tong, Giant flexomagnetoelectric effect in dilute magnetic monolayer, *Adv. Theory Simul.* **1**, 1800048 (2018).
- <sup>203</sup>F. Guinea, A. K. Geim and M. I. Katsnelson, Generating quantizing pseudomagnetic fields by bending graphene ribbons, *Phys. Rev. B* **81**, 035408 (2010).
- <sup>204</sup>J. Qi, X. Li and X. Qian, Bandgap engineering of rippled MoS<sub>2</sub> monolayer under external electric field, *Appl. Phys. Lett.* **102**, 173112 (2013).
- <sup>205</sup>J. Hong and D. Vanderbilt, First-principles theory of frozen-ion flexoelectricity, *Phys. Rev. B* **84**, 180101 (2011).
- <sup>206</sup>S. V. Kalinin, Y. Kim and D. D. Fong, Surface-screening mechanisms in ferroelectric thin films and their effect on polarization dynamics and domain structures, *Rep. Prog. Phys.* **81**, 036502 (2018).
- <sup>207</sup>A. N. Morozovska, E. A. Eliseev and M. D. Glinchuk, Ferroelectricity enhancement in confined nanorods: Direct variational method, *Phys. Rev. B* **73**, 214106 (2006).
- <sup>208</sup>E. A. Eliseev, I. S. Vorotiahin and Y. M. Fomichov, Defect-driven flexochemical coupling in thin ferroelectric films, *Phys. Rev. B* **97**, 024102 (2018).
- <sup>209</sup>M. S. Majdoub, P. Sharma and T. Cagin, Enhanced size-dependent piezoelectricity and elasticity in nanostructures due to the flexoelectric effect, *Phys. Rev. B* **77**, 125424 (2008).
- <sup>210</sup>F. Ahmadpoor and P. Sharma, Flexoelectricity in two-dimensional crystalline and biological membranes, *Nanoscale* **7**, 16555 (2015).

- <sup>211</sup>A. N. Morozovska, E. A. Eliseev and C. M. Scherbakov, Influence of elastic strain gradient on the upper limit of flexocoupling strength, spatially modulated phases, and soft phonon dispersion in ferroics, *Phys. Rev. B* **94**, 174112 (2016).
- <sup>212</sup>U. K. Roessler, A. N. Bogdanov and C. Pfleiderer, Spontaneous skyrmion ground states in magnetic metals, *Nature* **442**, 797 (2006).
- <sup>213</sup>A. N. Bogdanov and D. A. Yablonskii, Thermodynamically stable “vortices” in magnetically ordered crystals. The mixed state of magnets, *Zh. Eksp. Teor. Fiz.* **95**, 178 (1989).
- <sup>214</sup>H. J. Zhao, P. Chen and S. Prosandeev, Dzyaloshinskii–Moriya-like interaction in ferroelectrics and antiferroelectrics, *Nat. Mater.* **20**, 341 (2021).
- <sup>215</sup>K. C. Erb and J. Hlinka, Vector, bidirector, and Bloch skyrmion phases induced by structural crystallographic symmetry breaking, *Phys. Rev. B* **102**, 024110 (2020).
- <sup>216</sup>A. N. Morozovska, R. Hertel and S. Cherifi-Hertel, Chiral polarization textures induced by the flexoelectric effect in ferroelectric nanocylinders, *Phys. Rev. B* **104**, 054118 (2021).